NASA TECHNICAL NOTE

NASA TN D-5282

C. 1

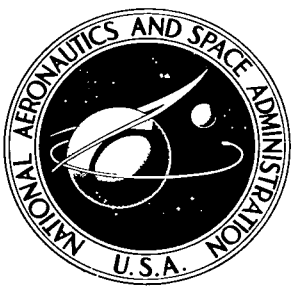

NASA TN D-5282

STEADY-STATE STRESS RELAXATION ANALYSIS OF TURBINE BLADE COOLING DESIGNS

by Albert Kaufman

Lewis Research Center

Cleveland, Ohio

NATIONAL AERONAUTICS AND SPACE ADMINISTRATION • WASHINGTON, D. C. • JUNE 1969

STEADY-STATE STRESS RELAXATION ANALYSIS OF TURBINE BLADE COOLING DESIGNS

By Albert Kaufman

Lewis Research Center
Cleveland, Ohio

NATIONAL AERONAUTICS AND SPACE ADMINISTRATION

For sale by the Clearinghouse for Federal Scientific and Technical Information
Springfield, Virginia 22151 – CFSTI price $3.00

ABSTRACT

An analytical evaluation was made of five turbine blade cooling configurations for advanced airbreathing engines on the basis of the time to a local creep strain of 1 percent for cast IN 100. The longest life was shown by the transpiration design (neglecting oxidation problems) followed by the multiple small hole design. Curves were established to predict the multiple small hole blade life under various combinations of turbine inlet and coolant temperatures and coolant to total gas flow ratios.

STEADY-STATE STRESS RELAXATION ANALYSIS OF TURBINE BLADE COOLING DESIGNS

by Albert Kaufman

Lewis Research Center

SUMMARY

An analytical evaluation was made of five turbine blade cooling configurations for advanced airbreathing engines on the basis of the steady-state operating times to 1 percent creep strain. The configurations consisted of a strut insert blade with horizontal fins, a film and convection cooled, a transpiration cooled, a multiple small hole, and a liquid metal cooled design. Analytical temperature distributions for a hypothetical Mach 3 supersonic cruise aircraft engine were used. The blades were assumed to operate under the centrifugal loading at cruise conditions of a typical first stage turbine rotor blade. Blade lives and stress and strain distributions were calculated by means of a stress relaxation computer program which used creep data for cast IN 100. The transpiration cooled design showed the longest operating life followed by the multiple small hole design. However, the latter was concluded to be more practicable for operation at high metal temperatures because of oxidation problems with the porous shell used in transpiration cooling. The superiority of the multiple small hole over the strut insert and film and convection cooled blades in the analysis was believed due largely to a more nearly optimum distribution of the coolant flow over the blade.

Design curves were established for the multiple small hole design to predict lives to 1 percent creep strain for various combinations of turbine inlet and coolant temperatures and coolant flow to total air flow ratios.

INTRODUCTION

Advanced airbreathing engines with high turbine gas inlet temperatures require cooling of the turbine blades. In this study, a number of cooling schemes have been

evaluated on the basis of the steady-state creep lives under supersonic cruise operating conditions.

Present blading materials are limited to metal temperatures of approximately 1800° F (1255 K) because of strength and oxidation considerations. However, for some engines the compressor discharge air which is the most convenient source for a coolant is already at a temperature above 1000° F (811 K). In order to utilize this coolant with a minimum amount of compressor bleedoff and cool the blade to within the limits on temperature levels and gradients set by the applied loads and the material strength and oxidation properties requires cooling configurations of high effectiveness.

A number of cooling schemes were analyzed from a heat transfer point of view in references 1 to 3. The engine operating conditions for this analysis were Mach 3, 75 000 feet (22.86 km), and a 2270° F (1517 K) gas turbine inlet temperature with a 1270° F (961 K) blade coolant inlet temperature. The blades had a chord width of about 2 inches (5.1 cm), a span length of 5.3 inches (13.46 cm), a hub to tip diameter ratio of 0.81, and were assumed to be fabricated from cast IN 100. Temperature distributions were determined analytically for a number of airfoil sections at various locations along the blade span; these results are reported in references 1 to 3. These blades were designed to sustain 1000 hours of steady-state operation based on three standard deviations of stress rupture properties and an empirical design procedure. In reference 4 cyclic lives based on a proprietary analysis were presented for sea level transient conditions.

The purposes of this study are threefold: (1) to present a method for examining various types of cooled blades under steady-state conditions taking into account the stress relaxation due to creep; (2) to investigate the steady-state lives of a number of different cooling configurations from references 1 to 3 using a stress relaxation method; and (3) to establish preliminary design curves for potential lives of the more promising of these configurations under various combinations of coolant flow ratio, coolant temperature, turbine inlet gas temperature, and centrifugal force.

In order to evaluate these designs, the centrifugal loads were based on operating conditions for a first stage rotor blade having a tip speed of 1243 feet per second (383 m/sec) and a hub-tip diameter ratio of 0.75. The steady-state operating lives to 1 percent creep strain were determined for five of the blade cooling configurations analyzed in references 1 to 3. These five schemes were (1) a strut inserted design where the midchord region is convectively cooled through horizontal fins, the leading edge is impingement cooled, and the coolant is discharged through a split trailing edge, (2) a film convection-cooled design where the midchord region is convection cooled and the leading and trailing edges are convection and film cooled, (3) a transpiration cooled design using a strut supported porous shell, (4) a multiple small hole design where the cooling is done primarily by film cooling by ejection of the coolant from the airfoil surface, and (5) a liquid metal cooled design. Temperature distributions from references 1 to 3 for an ap-

proximately 0.026 coolant to total gas flow ratio were used for this analysis.

The creep lives of these blade cooling configurations were calculated by means of a computer program which has the capability of taking into account the mechanical stresses from the external centrifugal and gas loads, the thermal stresses due to the temperature gradients, and the redistribution of stresses with time because of creep. One effect of creep is to cause a relaxation of the high thermal stresses. If this relaxation is ignored the predicted blade life will be too pessimistic. On the other hand, if the thermal stresses are ignored entirely the predicted blade life will be too optimistic. Therefore, a stress relaxation analysis is required to realistically evaluate blade life.

The analysis does not consider effects of damage due to thermal fatigue, vibrations, impact, or erosion. Some or all of these effects can occur at various times during the service lives of turbine blades under engine design, takeoff, and off-design conditions. The actual blade lives will depend on the interaction of all these factors with the steady-state conditions. Even if the magnitudes of all these nonsteady-state effects were known, a prediction of blade lives combining these effects with the steady-state effects is beyond the current state of the art.

Under steady-state conditions, the elapsed time to obtain 1 percent creep strain (henceforth called creep life), the initial and final stress distributions, and the final strain distributions are presented for each design. Creep lives for these designs are compared on the basis of the initially (prior to stress relaxation) worst combination of stress and temperature, the centrifugal stress and the average temperature, and the effect of creep as determined from the stress relaxation computer program.

Conclusions are drawn as to the high temperature capabilities of these designs. Design curves are established in order to evaluate the effect on the creep life of the multiple small hole configuration of various combinations of coolant temperature, turbine inlet gas temperature, cooling air flow to total gas flow ratio, and centrifugal force.

SYMBOLS

A	area, $in.^2$; m^2
C_1, C_2, C_3	coefficients defining a plane
E	modulus of elasticity, psi; N/m^2
F	centrifugal force, lb; N
k	curve fix constants
L	span length, in.; m
M	bending moment with respect to original axis, lb-in.; N-m

M'	bending moment with respect to centroidal axis, lb-in.; N-m
n	number of nodes
R	radius of curvature, in.; m
T	temperature above 70^{o} F, ^{o}F; K
T_R	temperature, ^{o}R; K
t	time, hr
w	deflection, in.; m
x	distance along x axis, in.; m
$\bar{x}$	distance to centroid in direction of x axis, in.; m
x'	distance along x' centroidal axis, in.; m
y	distance along y axis, in.; m
$\bar{y}$	distance to centroid in direction of y axis, in.; m
y'	distance along y' centroidal axis, in.; m
z	distance along z axis, in.; m
α	coefficient of thermal expansion, in./in./^{o}F; m/m/K
ϵ	strain, in./in.; m/m
θ	angle between x' and x axes, rad
σ	stress, psi; N/m^2

Subscripts:

c	creep
k	node index
o	hub
p	plastic
t	total
x, y, z	with respect to x, y, z axes, respectively

ANALYTICAL CONDITIONS

Cooling Configurations

The five cooling schemes that were analyzed are illustrated in figures 1 to 5. In the strut insert design of figure 1, air flows up the central cavity formed by the strut insert and through holes at the leading edge of the insert to impingement cool the blade leading edge. The air then circulates through horizontal fins between the shell and strut and discharges through slots in the trailing edge. For the purpose of this analysis, the outer shell, strut, and horizontal fins are assumed to be integral.

The film and convection cooled design of figure 2 has the cooling air injected through the blade base into two central and one leading edge cavities. The air then circulates up and down a series of vertical passages. At the leading edge the air passes through small holes in the wall of the adjacent vertical passage, impinges on the internal leading edge surface, and discharges through film cooling holes. The trailing edge is convectively cooled by air discharging through slots.

The transpiration cooled design of figure 3 has a shell of wire-form porous material attached to a strut which carries the shell. Air flows up the central plenum of the hollow strut, through metering holes to the strut surface which consists of a waffle-like pattern of cavities, and then through the porous shell. The shell material is cooled by a combination of convection and film cooling which is highly effective because of the many fine pores through the shell structure.

The multiple small hole design of figure 4 is essentially a film cooling scheme which employs a large number of closely spaced holes in the shell wall. These holes are considerably larger than the pores in the fine wire mesh used in the transpiration cooled design of figure 3 and are, therefore, less susceptible to clogging because of metal oxidation at high temperatures. In the multiple small hole design the shell is stiffened by cross ribs and is capable of supporting itself under engine operating conditions without a strut.

In the design shown in figure 5, the leading edge and midchord regions are convectively cooled by employing a liquid metal; in this case, potassium. Boiling of the potassium occurs as it flows through radial passages inside the airfoil part of the blade. Condensation occurs below the blade platform in heat exchangers which are cooled by compressor discharge air. The trailing edge is convectively air cooled.

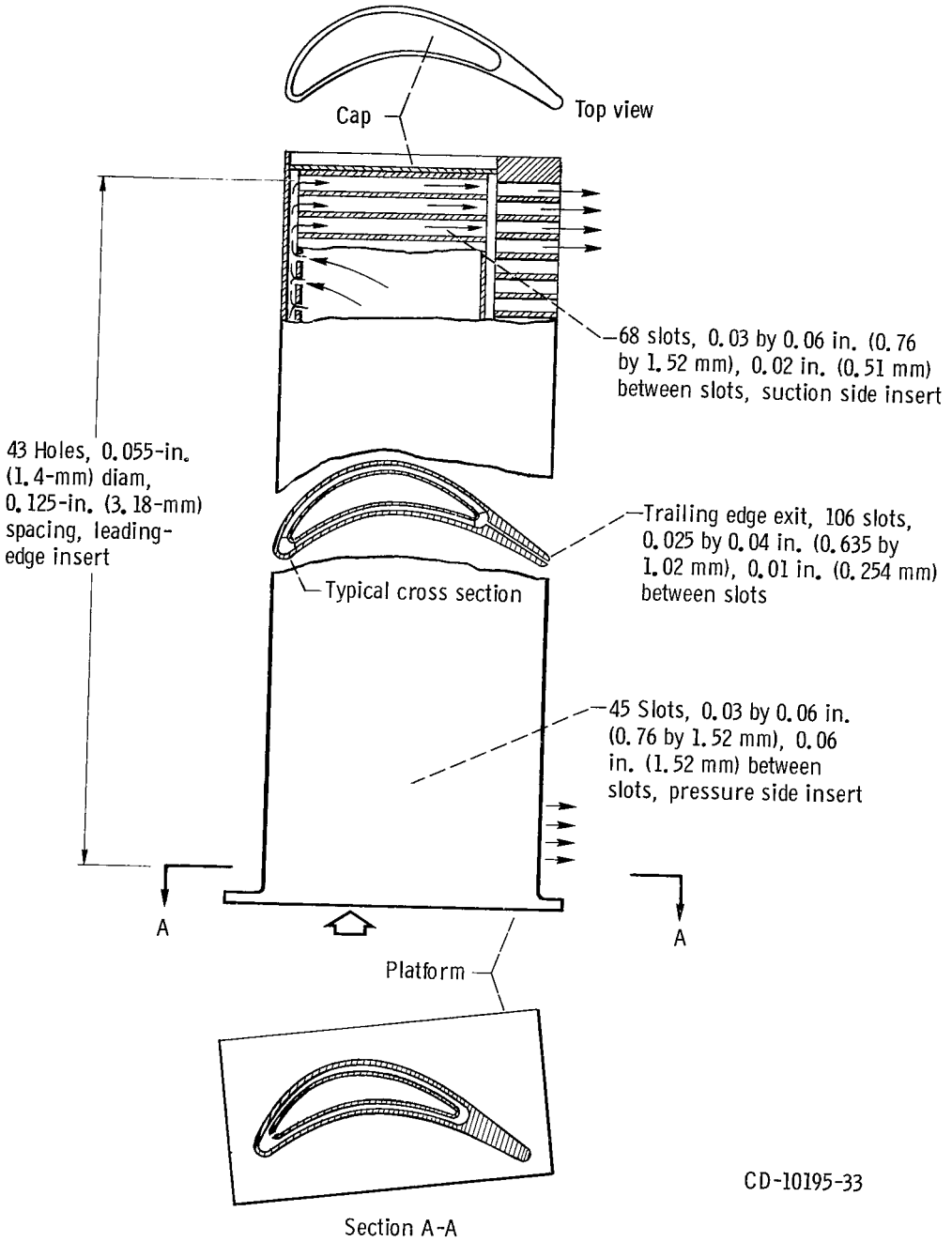

Figure 1. - Strut insert design.

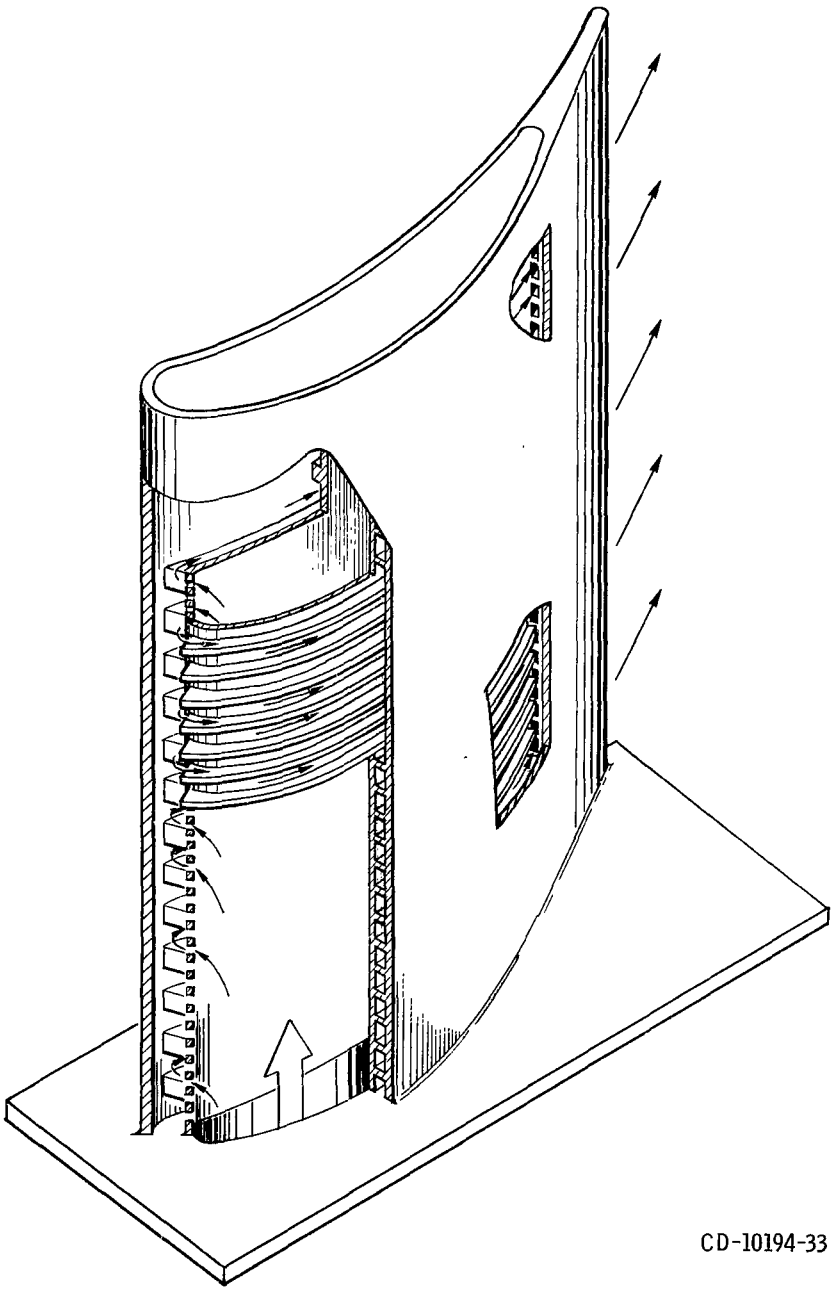

CD-10194-33

Figure 1. - Concluded.

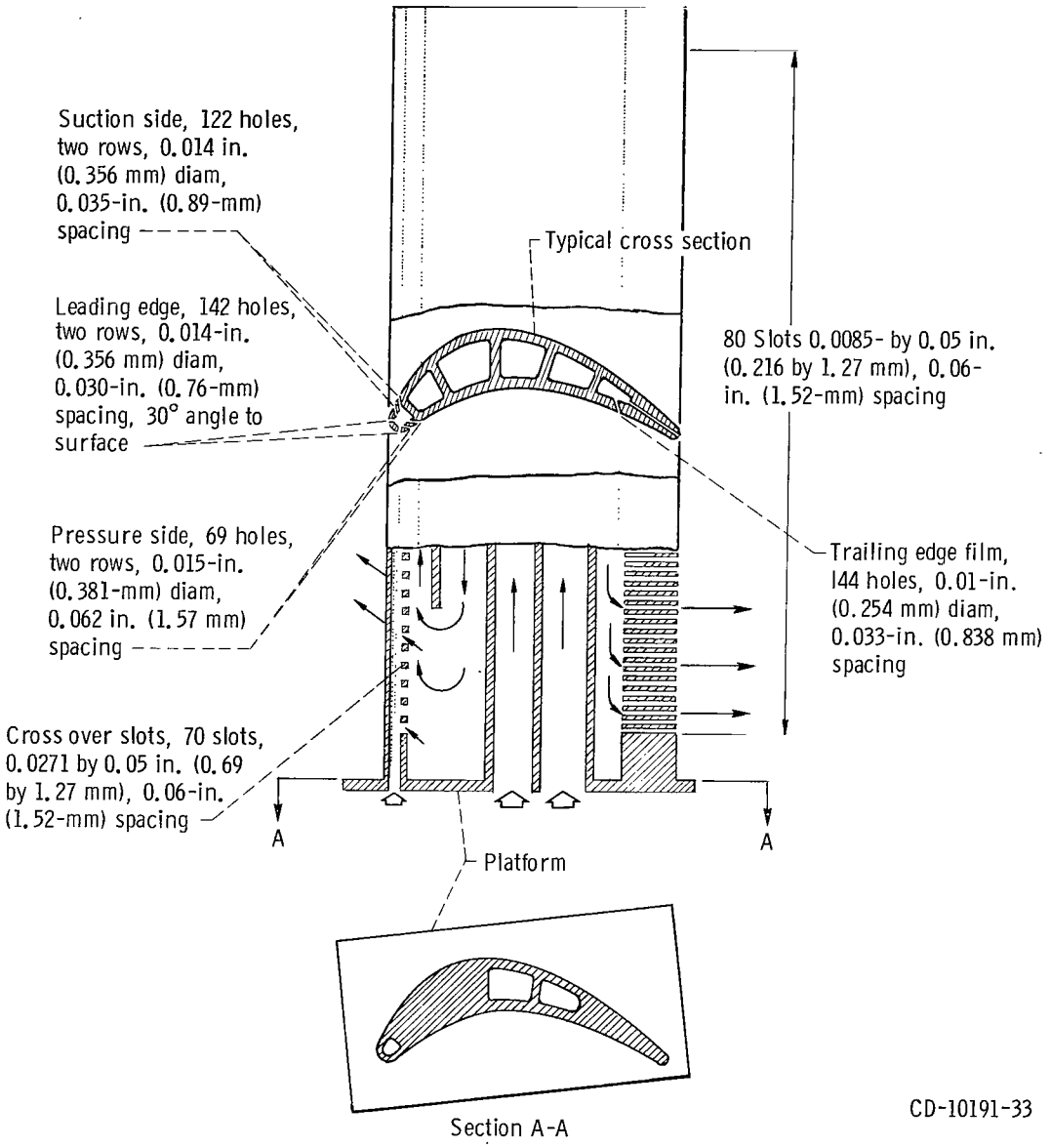

Figure 2. - Film-convection cooled design.

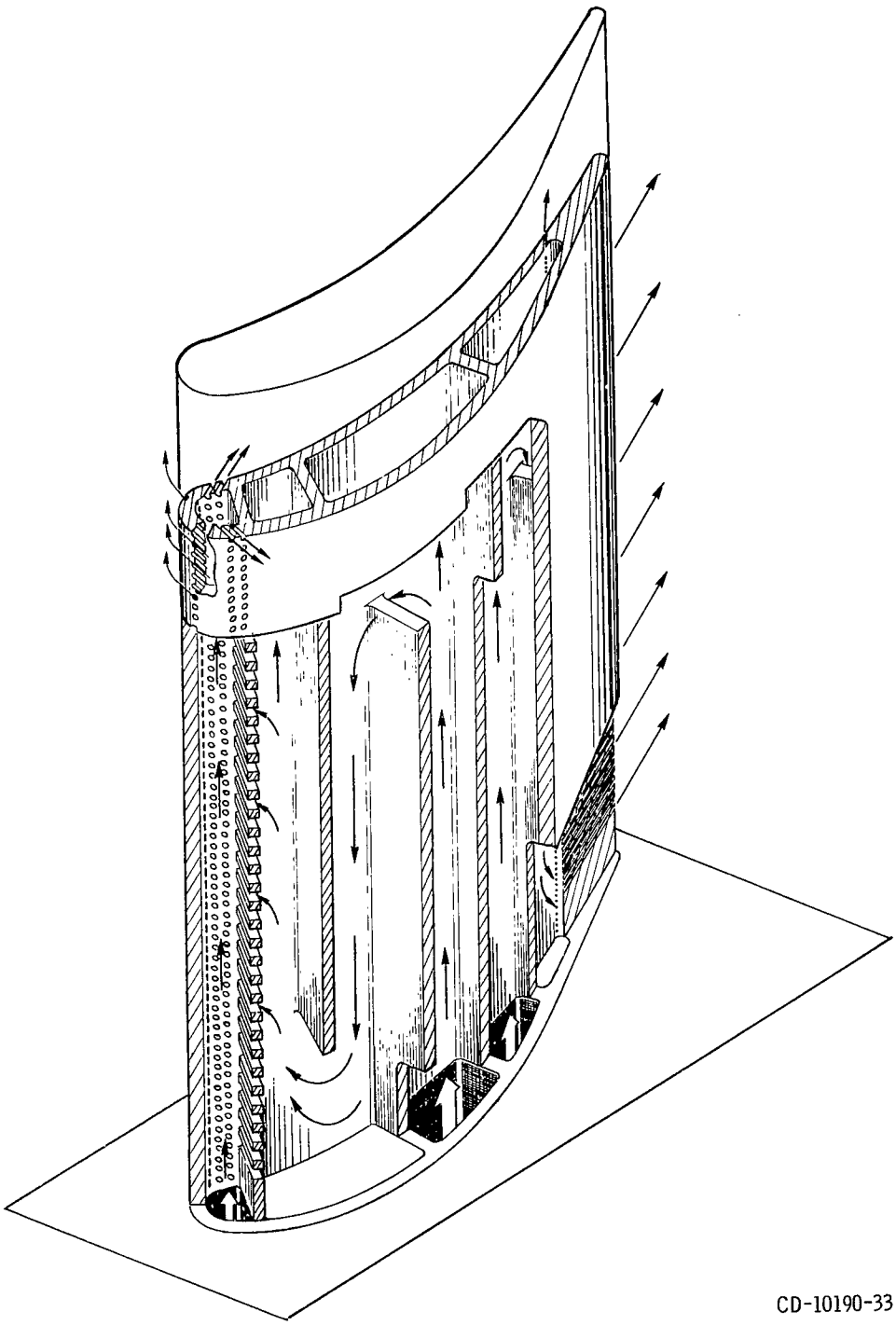

CD-10190-33

Figure 2. - Concluded.

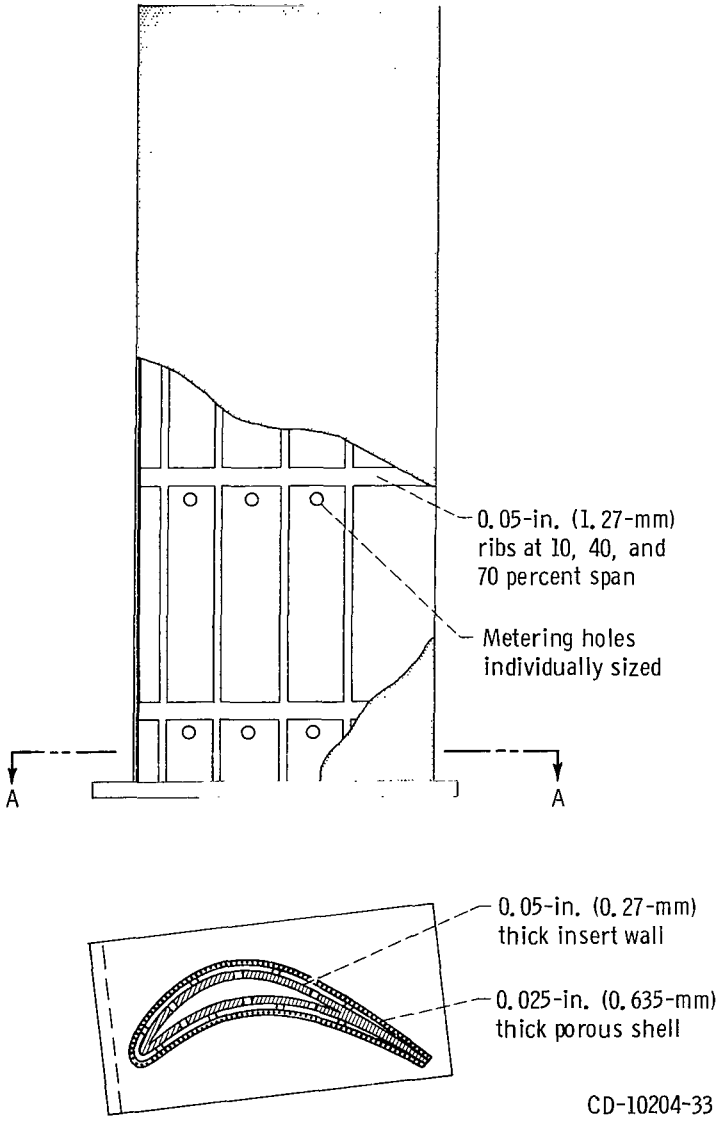

Figure 3. - Transpiration-cooled design.

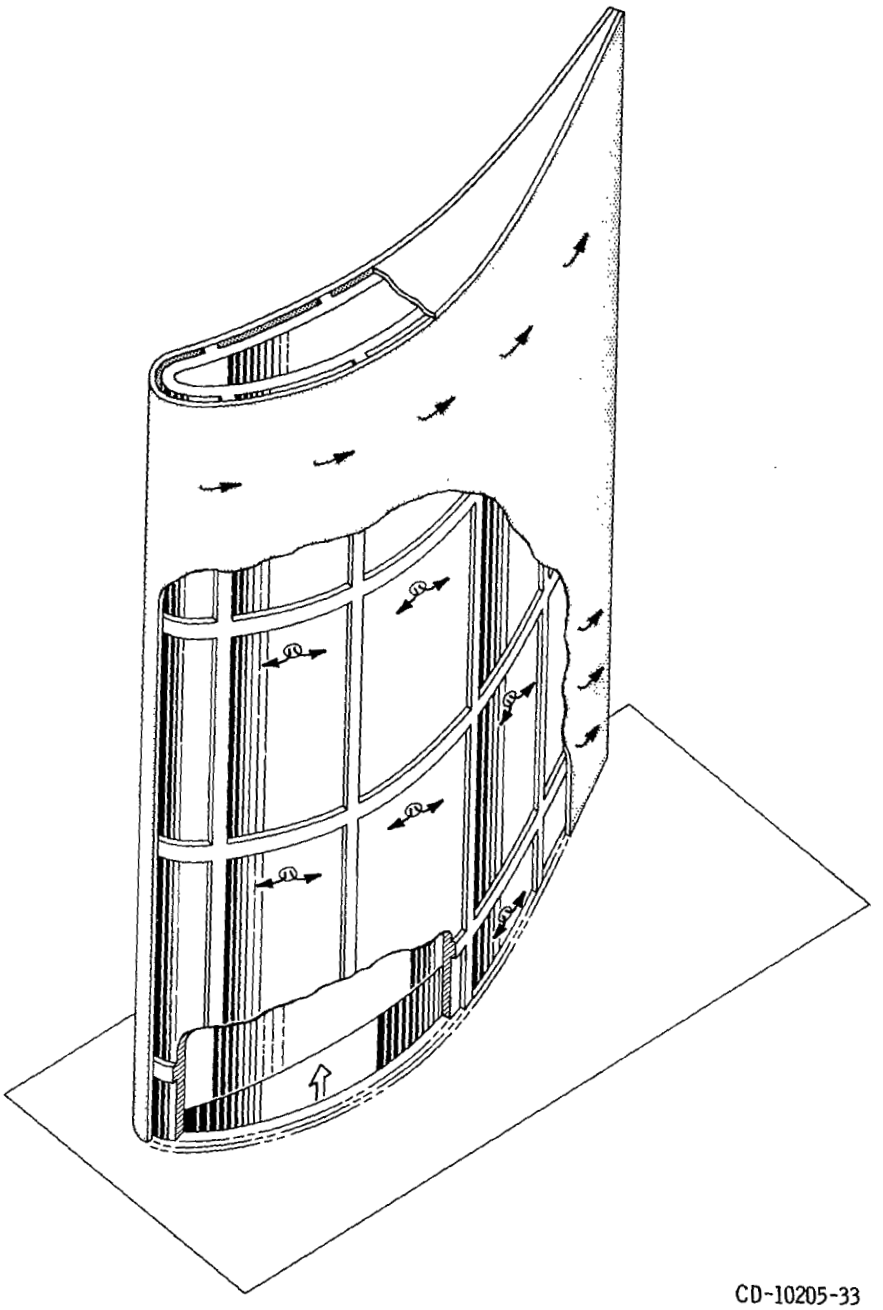

CD-10205-33

Figure 3. - Concluded.

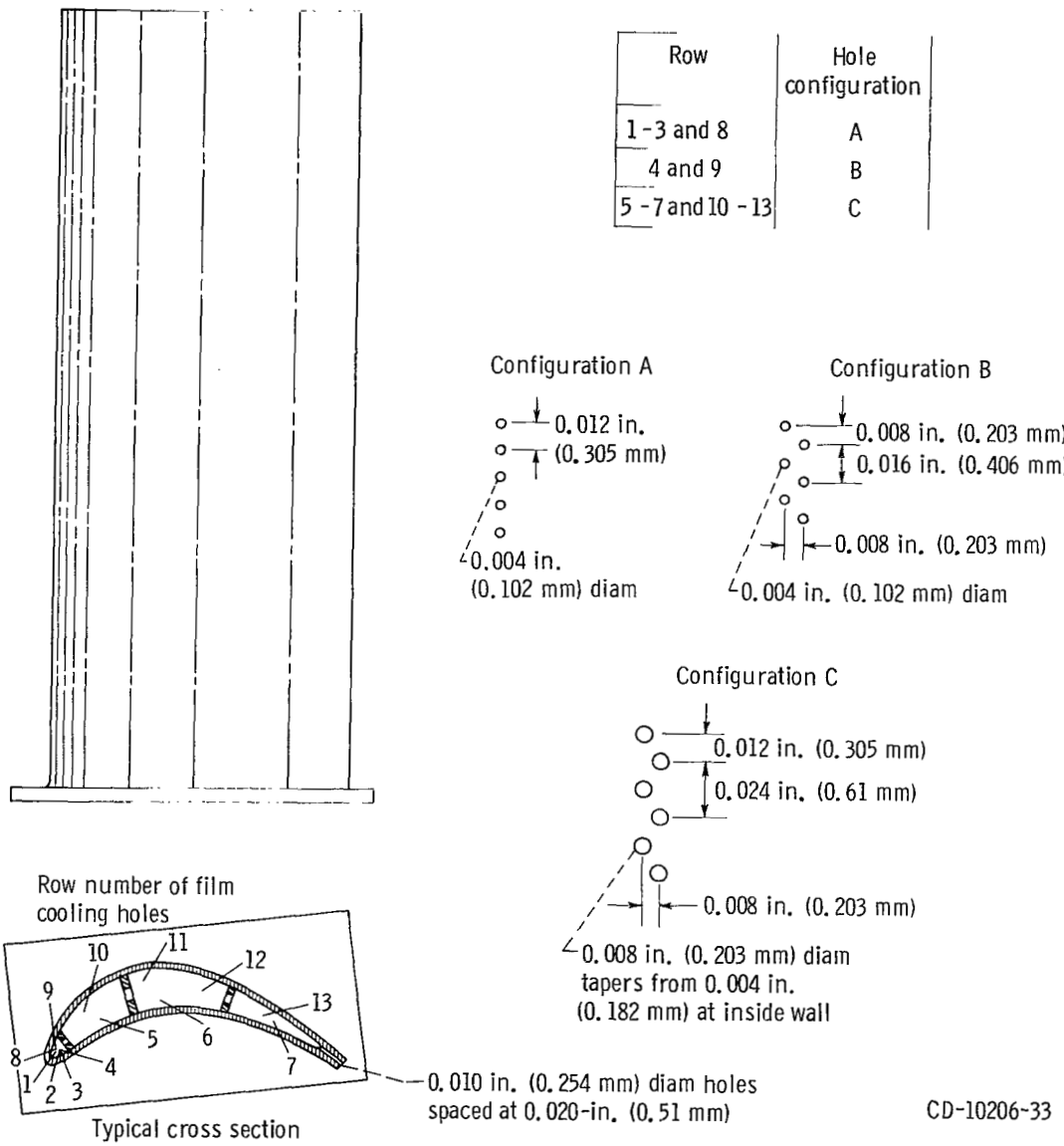

Figure 4. - Multiple small-hole design.

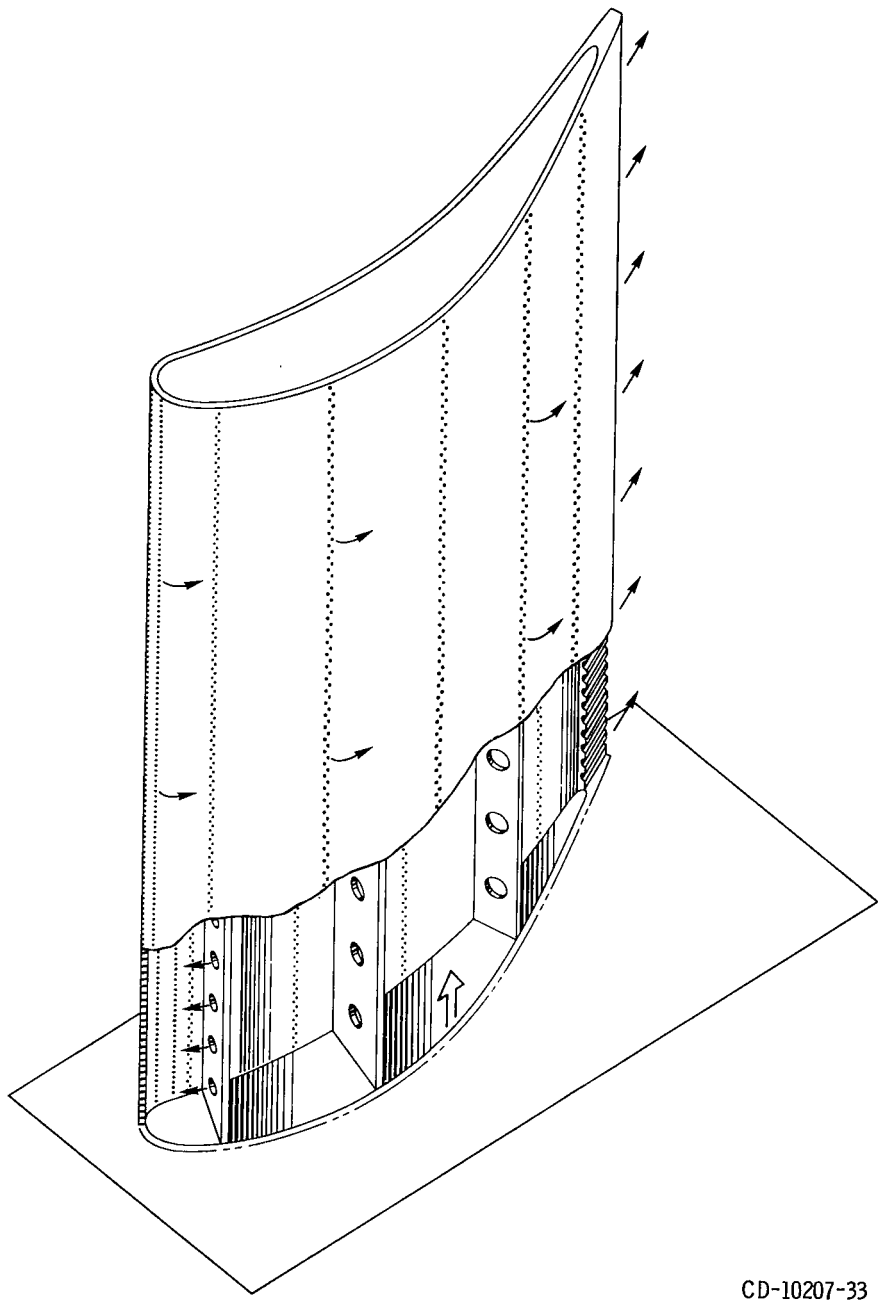

CD-10207-33

Figure 4. - Concluded.

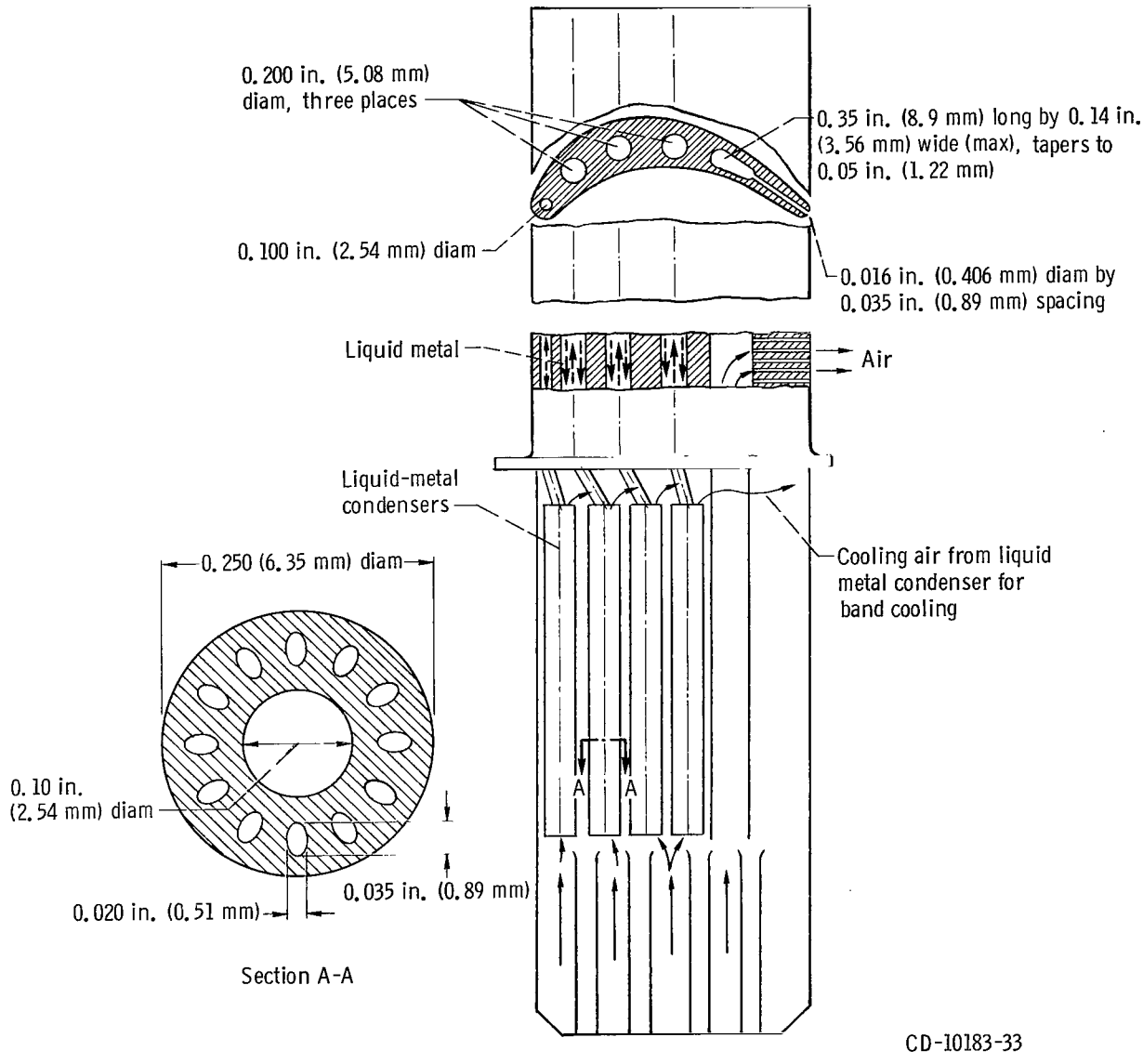

Figure 5. - Liquid-metal- and convection-cooled design.

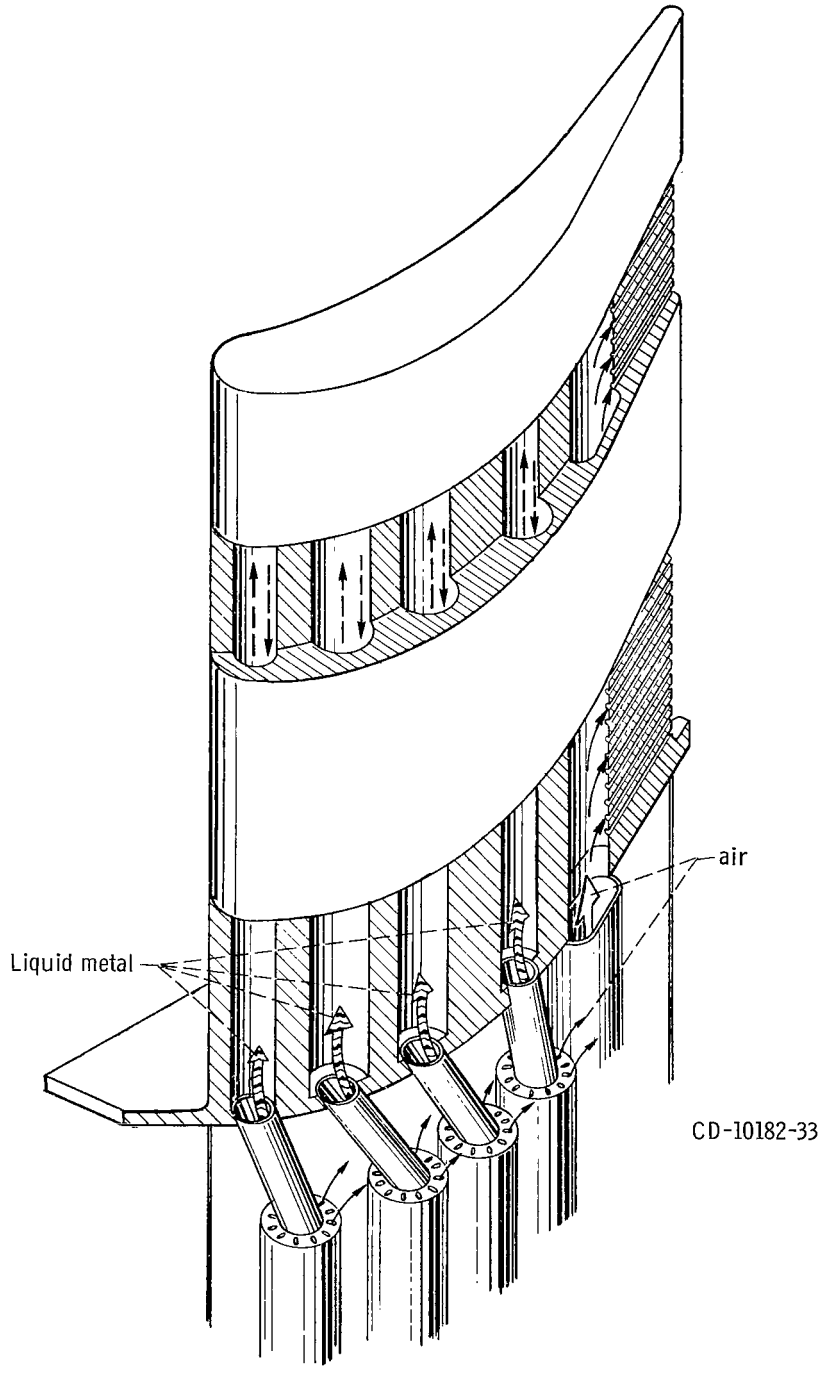

Figure 5. - Concluded.

Temperatures

The heat transfer analysis of references 1 to 3 was done for operating conditions as found in an advanced airbreathing engine with a 2270° F (1517 K) turbine inlet temperature at Mach 3 and 75 000 feet (22 859 km) altitude. The blade material was assumed cast IN 100. The heat transfer calculations of references 1 to 3 cover a wide range of coolant flow ratios. In order to arrive at a uniform basis for comparing the designs, coolant flow ratios of approximately 0.026 were selected. In the case of the multiple small hole design where no results were presented for a 0.026 coolant flow ratio, the temperature distributions were obtained by averaging the results for 0.0286 and 0.0223 coolant flow ratios.

A survey was made to determine the critical span location for each design by calculating a nominal stress rupture life based on the average temperature at the section and the centrifugal stress distribution. The average temperatures were obtained from the temperature distributions which were given for each configuration at various span locations in references 1 to 3. It was found that in all cases the hub was critical when the temperature distribution at the section closest to the hub section of the airfoil was considered to apply at the hub also. These sections were 8 to 20 percent of the span distance from the airfoil base. The only exception to this was in the case of the transpiration cooled design where strut temperatures were only presented for the 60 percent span section. Since the strut is the load carrying member and the shell temperatures showed little variation with span distance, the 60 percent span temperature distribution was also applied to the hub section of the strut. This was a conservative approach since the hub section of the strut would be cooler than the 60 percent span section. The complete temperature distributions were given in references 1 to 3 for one section only, usually in the vicinity of the midspan. At other sections, metal temperatures were given at approximately 15 points. Temperatures at intermediate locations for the purpose of this analysis were obtained by a combination of interpolation and the use of the midspan temperature distribution as a guide. The temperatures that were used from references 1 to 3 are shown in figures 6 to 10 for each design.

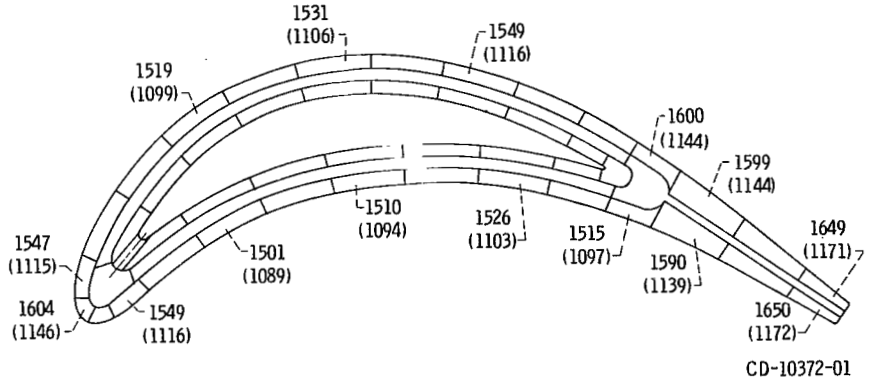

Figure 6. - Temperature distribution for strut insert design.

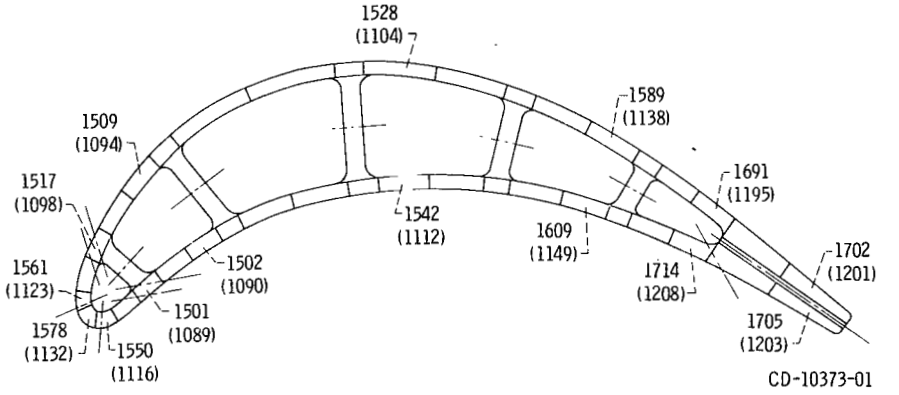

Figure 7. - Temperature distribution for film-convection-cooled design.

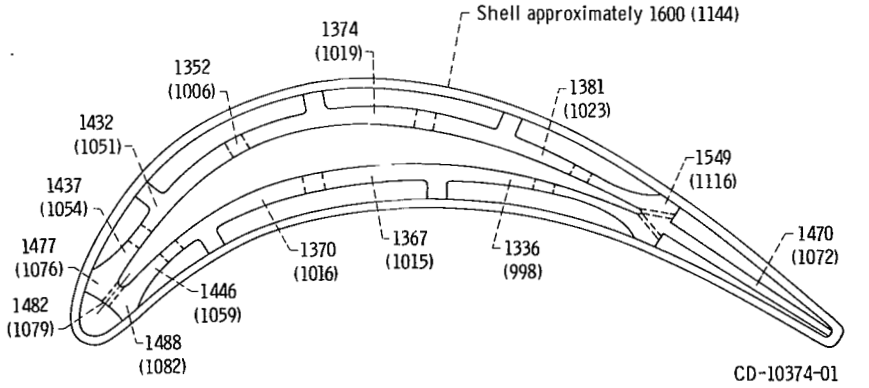

Figure 8. - Temperature distribution for transpiration-cooled design.

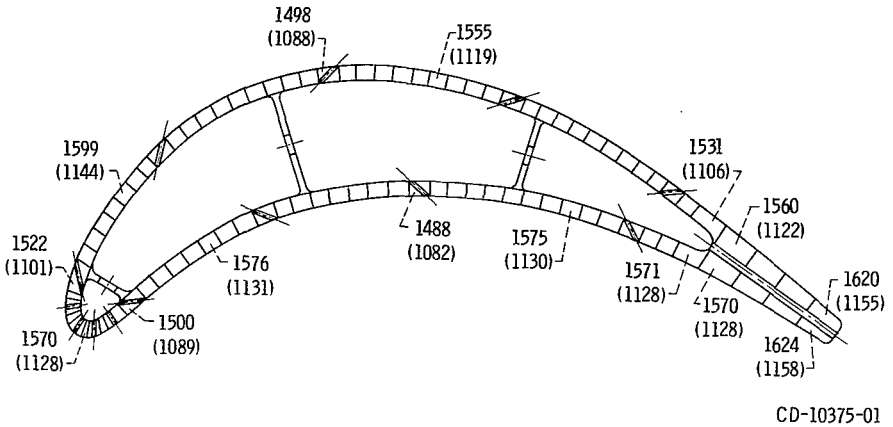

Figure 9. - Temperature distribution for multiple small-hole design.

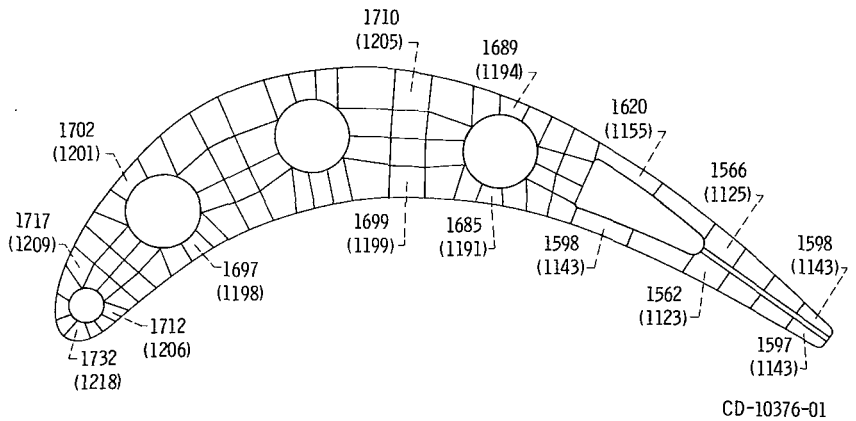

Figure 10. - Temperature distribution for liquid-metal- and convection-cooled design.

Applied Loads

For purposes of evaluating these configurations the centrifugal loads were based on the operating conditions and the geometry of a first stage turbine blade with a tip speed of 1243 feet per second (383 m/sec) and a hub-tip diameter ratio of 0.75. From analyses of similar configurations for the same turbine rotor blades, average centrifugal stresses of 31 000, 29 000, 37 000, and 30 000 psi (21 374, 19 995, 25 511, and 20 684 N/cm^2) were assigned to the strut insert, film and convection cooled, transpiration cooled, multiple small hole, and liquid metal and convection cooled designs, respectively. These stresses were applied to the airfoil sections closest to the airfoil base, hereafter called hub sections. The effect of bending moments due to the gas forces was neglected in this analysis because it was assumed these would be cancelled out by tilting

the blades. However, bending moments due to the offsetting of the line of action of the centrifugal force as a result of blade bending due to creep were considered.

ANALYTICAL PROCEDURE

Stress distributions in the airfoil sections were calculated by a stress relaxation procedure which is explained in detail in appendix A. This general program takes into account the applied loading on the blade, thermal stresses, and creep effects under steady-state operation. In accordance with present practice beam theory is used; that is, plane sections are assumed to remain plane. The program has the capability of treating instantaneous plastic flow or residual stress effects. However, all the stresses were in the elastic range for all the cases considered in this investigation.

In appendix B a procedure is suggested for determining the effect of creep on the bending moments. The effect of these moments was approximated by (1) assuming the deflection distribution over the blade span as a function of the slope (C_2 or C_3 in eq. (A1)) of the hub section on the assumption of small deformation, (2) determining the centrifugal force distribution over the span for a normal tapered airfoil shell, and (3) calculating the total restoring moment on the hub section as a function of the slope by multiplying (1) and (2) and integrating the results.

The analysis does not consider the effects of nonlinear spanwise temperature gradients. In the cases of the transpiration cooled blade where the strut was assumed to be at a constant temperature and the multiple small hole blade where the spanwise variation of average section temperatures was fairly linear the analysis of appendix A is reasonably accurate. The other configurations also had fairly linear spanwise temperature gradients in references 1 to 3 except near the tip where the temperatures leveled off or decreased rather sharply. The effects these have on the accuracies of the calculations are unknown.

The basic nodal breakup of the airfoil sections for each configuration as shown in references 1 to 3 was used for this investigation. However, the strut for the transpiration cooled design had to be divided into small area elements since no nodal breakup was given for it in references 1 to 3. Distances from the centroids of each of these nodes to an arbitrary set of coordinate axes were determined. Temperatures based on the heat transfer analyses were assigned to each node. The material properties are tabulated in the program as functions of temperature and are, therefore, known at each node.

Creep data were obtained for IN 100 alloy from the International Nickel Company for creep strains of 0.1, 0.2, 0.5, and 1.0 percent at temperatures of 1350°, 1500°, 1700°, 1800°, and 1900° F (1005, 1089, 1200, 1255, and 1311 K) and times from 10 to 1000 hours. These creep data were correlated using a Larson-Miller parameter as shown in

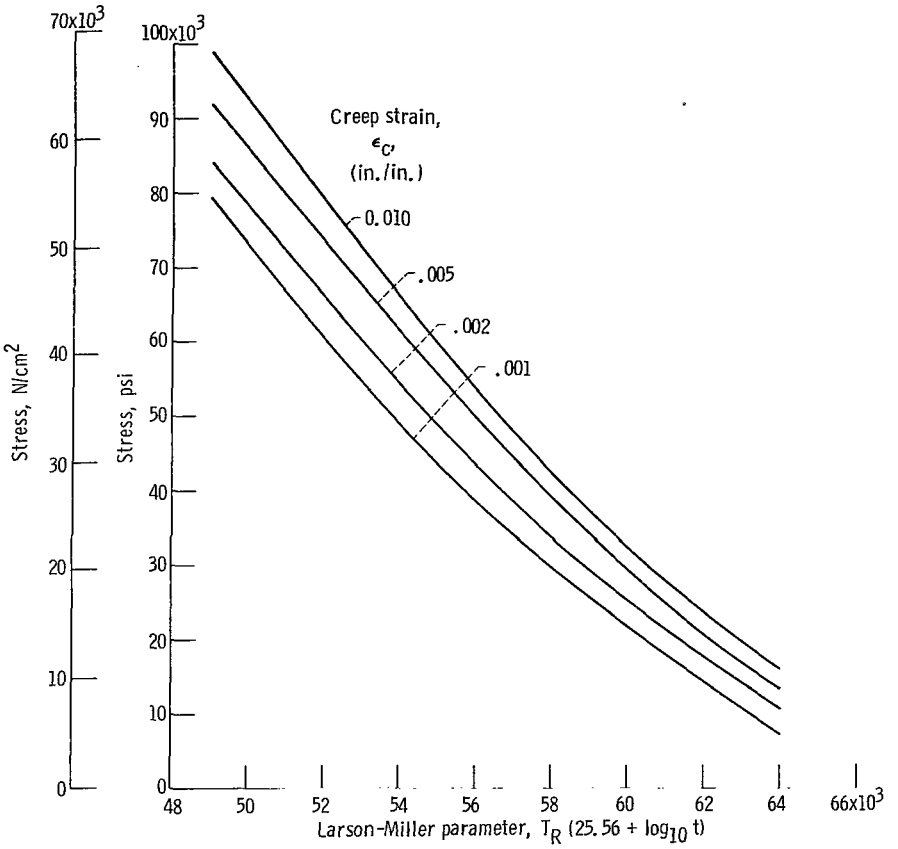

Figure 11. - Creep data correlation for IN 100.

figure 11. The parametric constant was optimized from the available data by using the computer program described in reference 3. It was assumed that compressive stresses produce compressive creep strains of the same magnitude as the tensile stresses for any given absolute stress, time, and temperature. An equation of the form

$$\log_{10} t_c = k_1\sigma + \left[k_2\sigma + k_3\right]\left[T_R(25.56 + \log_{10} t)\right] + k_4 \qquad (1)$$

was fitted to the creep curves of figure 11.

A strain hardening rule was used to determine cumulative creep strains. This procedure and the application of the rule are explained in appendix A.

RESULTS AND DISCUSSION

Creep Lives

The creep lives to 1 percent creep strain are shown in table I for the Mach 3, 75 000 feet (22.859 km), 2270° F (1517 K) turbine inlet temperature, and 1270° F (961 K) blade coolant inlet temperature conditions. In addition to the results from the stress relaxation analysis shown in the third and fourth columns, creep lives are given for the worst combination of stress and temperature using initial conditions (0 hr at the steady-state conditions) in the second column and for the average temperature and stress at the hub section for each blade design in the last column. Creep lives from the stress-relaxation analysis are presented with and without the effect of restoring moments due to centrifugal force being considered.

Since the creep correlation curves of figure 11 were based on data from 10 to 1000 hours, results outside this range and, particularly, beyond 10 000 hours can be considered as only qualitatively significant. More accurate creep lives could have been obtained if the Larson-Miller correlation had covered creep data in the 1000- to 100 000-hour range. Because of this deficiency in the creep data correlation, the results shown in table I are used only to compare designs and describe trends.

The blade creep lives of various designs based on the stress relaxation analysis with restoring moments being considered were, in descending order: (1) the transpiration cooled design with an infinite life; (2) the multiple small hole design with 11 600 hours; (3) the strut insert design with 7200 hours; (4) the film and convection cooled de-

TABLE I. - RESULTS OF CREEP LIFE ANALYSES

[Cruise speed, Mach 3; cruise altitude, 75 000 ft (22.859 km); turbine inlet temperature, 2270° F (1517 K); blade inlet coolant temperature, 1270° F (961 K).]

Blade cooling design	Time to 1 percent creep strain, hr			
	Based on initial conditions	Based on stress relaxation analysis		Based on average conditions
		Uncorrected for restoring moment due to centrifugal force	Corrected for restoring moment due to centrifugal force	
Strut insert	2430	4 700	7 200	47 900
Film convection	186	1 750	2 850	46 700
Transpiration	2530	47 900	Infinite	Infinite
Multiple small hole	4800	8 600	11 600	33 500
Liquid-metal convection	68	130	134	498

sign with 2850 hours; and (5) the liquid metal and convection cooled design with 134 hours.

The effect of the restoring moments was to cause an increase in the creep lives. The reason for this is that it counters the tendency of the blade section to rotate due to creep. The life of the transpiration cooled design increased from 47 900 hours to an infinite life while that of the liquid metal design increased only slightly due to the restoring moments. However, the qualitative ranking of the blade designs in terms of creep life did not change.

The reason for the superiority of the transpiration cooled design was that the strut had a relatively low average temperature of about 1400° F (1033 K) which more than compensated for the high centrifugal stress level required to support the porous shell. Similarly, the liquid metal design had such low life because the hub section was at an average temperature of 1659° F (1177 K). Since the other three designs had approximately the same centrifugal stresses (29 000 to 31 000 psi or 19 995 to 21 374 N/cm^2) and average hub temperatures (approximately 1570° F (1127 K)), their creep lives should depend largely on the maximum chordwise temperature differences.

As can be seen by comparing figures 6, 7, and 9, the strut insert design has about a 10 percent higher temperature difference and the film-convection design has about a 60 percent higher temperature difference than the multiple small hole design at the hub. Therefore, one would expect the multiple small hole design to be the best of the three and the film convection design the worst as is indeed the case.

As expected, the creep lives based on the initial conditions were too pessimistic while those based on the average conditions were too optimistic. Neither gave the same ranking of designs as the stress relaxation analysis. The stress relaxation effects cannot be determined from a mere inspection of the initial conditions because creep rates varied throughout the blade section and changed as the stresses become redistributed. Furthermore, the critical location where the worst creep occurs sometimes changed because of the stress relaxation.

The relative merit of the designs cannot be determined by neglecting the thermal stresses and considering only the mechanical stresses and the average temperature levels. Thus, on the basis of the average conditions, the film-convection cooled design appeared better than the multiple small hole design in table I whereas the stress relaxation analysis showed the reverse to be true.

Stress and Strain Distributions

In figures 12 to 16 the initial stress distributions and the final stress distributions at the hub sections at the time when 1 percent creep strain or 100 000 hours was reached

are shown in part (a) and the final creep strain distributions are shown in part (b). Since the tolerance of the blade material to any stress level is a function of temperature the critical location is determined from the creep strain distribution in part (b) of figures 12 to 16.

Strut insert design. - The stresses in the strut insert were higher than those in the shell and the stresses in the pressure side of the shell were higher than in the suction side, as shown in figure 12(a). However, significant stress relaxation occurred in these regions with compensating increases in the stresses on the shell leading edge and suction side.

Considerably more creep strain took place toward the trailing edge than the leading edge. The 1-percent creep strain was reached at the extreme trailing edge (fig. 12(b)). This design as well as others that showed unbalanced creep strain distributions at the hub section would be improved by a more uniform wall temperature distribution. In this case, the creep life could be somewhat increased by letting the leading edge run hotter and reducing the metal temperature at the trailing edge. Sometimes this may be difficult to do without adversely affecting the blade life at some other location. For example, with most of the blades considered the leading edge was critical at the midspan location and any further increase in temperature at that position would probably have a deleterious effect on the low cycle fatigue life.

Film and convection cooled design. - The webs were the coolest parts of the film-convection blade and, therefore, had the highest stresses. Some relaxation of these stresses is shown in figure 13(a). In addition, the final stress distribution showed a reduction of the trailing edge stresses. Even with this stress relaxation the trailing edge remained critical. The final creep strain distribution of figure 13(b) was radically unbalanced with most of the creep occurring at the trailing edge.

In order to investigate the effect of the web temperature on the creep life, another version of this blade was analyzed in which the web temperatures were arbitrarily made the same as the temperatures at the adjoining parts of the shell. This lowered the web stresses but did not significantly affect those at the trailing edge which remained critical. The raising of the web temperatures also increased the average temperature level of the hub section slightly. This resulted in a slower stress relaxation at the trailing edge which reached 1 percent creep in 1300 hours compared to the 1750 hours for the original design (without restoring moments being considered).

The creep life from the stress relaxation analysis was about 15 times that based on initial conditions compared to a factor of about 3 for the strut insert design in table I. This was due to the fact that the initial critical location for the film-convection design was at a highly stressed web node which relaxed rapidly and moved the final critical location to the trailing edge. In contrast, the critical region of the strut insert design remained around the trailing edge which showed little relaxation in figure 12(a).

Key	Stress		Creep strain,	Key	Stress		Creep strain,
	psi	(N/cm^2)	in./in.		psi	(N/cm^2)	in./in.
0	Under 15 000	(Under 10 342)	Under 0.001	5	35 000 to 40 000	(24 132 to 27 579)	0.005 to 0.006
1	15 000 to 20 000	(10 342 to 13 790)	0.001 to 0.002	6	40 000 to 45 000	(27 579 to 31 026)	.006 to 0.007
2	20 000 to 25 000	(13 790 to 17 237)	.002 to 0.003	7	45 000 to 50 000	(31 026 to 34 474)	.007 to 0.008
3	25 000 to 30 000	(17 237 to 20 684)	.003 to 0.004	8	50 000 to 55 000	(34 474 to 37 921)	.008 to 0.009
4	30 000 to 35 000	(20 684 to 24 132)	.004 to 0.005	9	55 000 to 60 000	(37 921 to 41 368)	.009 to 0.010
				*	----------	----------	Above 0.010

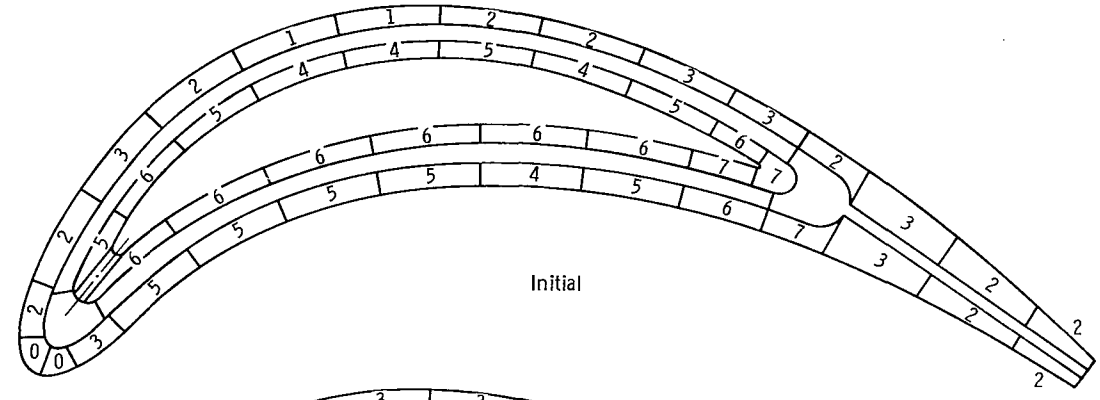

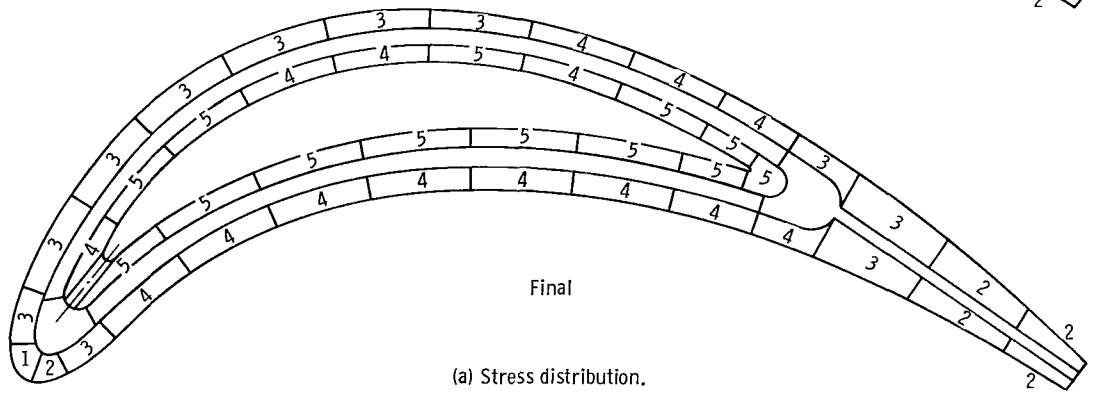

(a) Stress distribution.

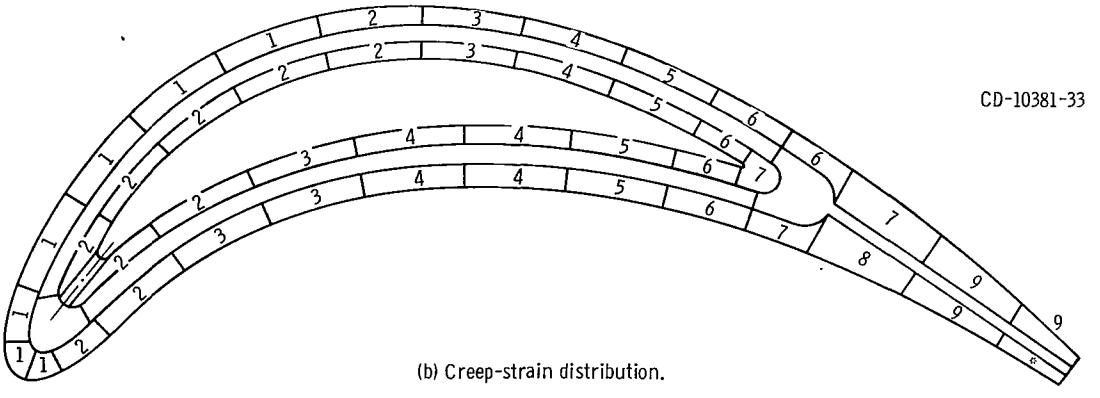

(b) Creep-strain distribution.

Figure 12. - Stress analysis results for strut insert design.

Key	Stress		Creep strain,	Key	Stress		Creep strain,
	psi	(N/cm^2)	in./in.		psi	(N/cm^2)	in./in.
0	Under 15 000	(Under 10 342)	Under 0.001	5	35 000 to 40 000	(24 132 to 27 579)	0.005 to 0.006
1	15 000 to 20 000	(10 342 to 13 790)	0.001 to 0.002	6	40 000 to 45 000	(27 579 to 31 026)	.006 to 0.007
2	20 000 to 25 000	(13 790 to 17 237)	.002 to 0.003	7	45 000 to 50 000	(31 026 to 34 474)	.007 to 0.008
3	25 000 to 30 000	(17 237 to 20 684)	.003 to 0.004	8	50 000 to 55 000	(34 474 to 37 921)	.008 to 0.009
4	30 000 to 35 000	(20 684 to 24 132)	.004 to 0.005	9	55 000 to 60 000	(37 921 to 41 368)	.009 to 0.010
				*	----------	----------	Above 0.010

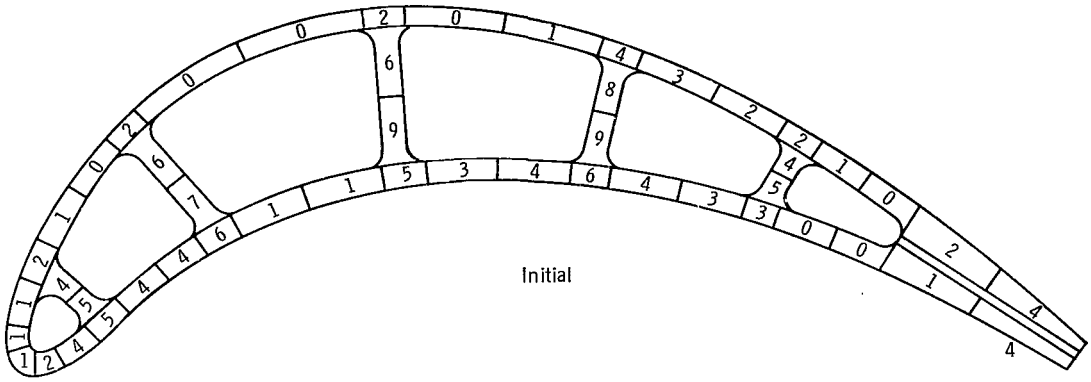

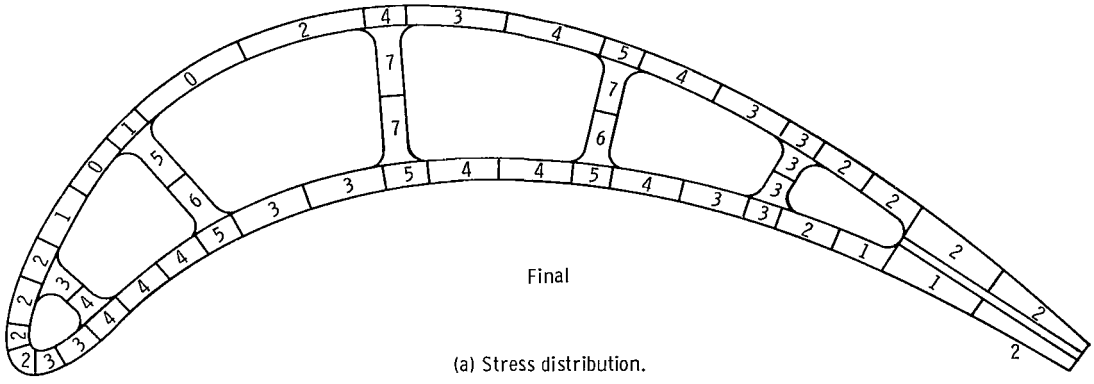

(a) Stress distribution.

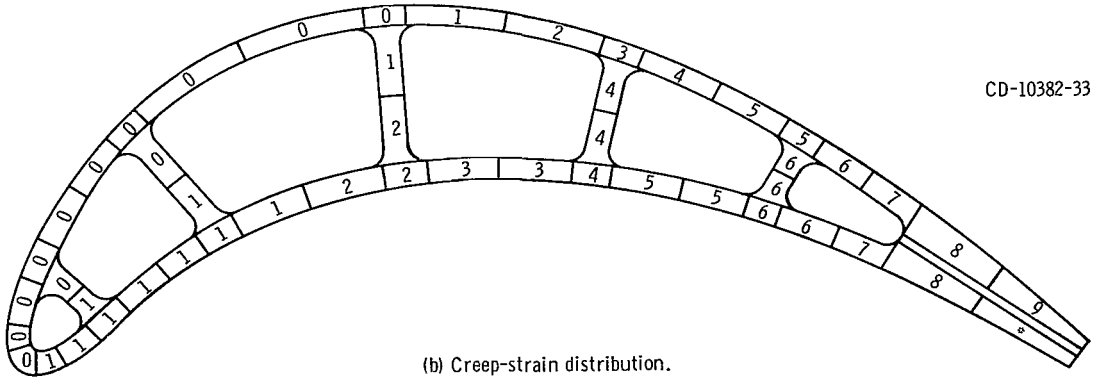

CD-10382-33

(b) Creep-strain distribution.

Figure 13. - Stress analysis results for film-convection cooled design.

Key	Stress		Creep strain,	Key	Stress		Creep strain,
	psi	(N/cm^2)	in./in.		psi	(N/cm^2)	in./in.
0	Under 15 000	(Under 10 342)	Under 0.001	5	35 000 to 40 000	(24 132 to 27 579)	0.005 to 0.006
1	15 000 to 20 000	(10 342 to 13 790)	0.001 to 0.002	6	40 000 to 45 000	(27 579 to 31 026)	.006 to 0.007
2	20 000 to 25 000	(13 790 to 17 237)	.002 to 0.003	7	45 000 to 50 000	(31 026 to 34 474)	.007 to 0.008
3	25 000 to 30 000	(17 237 to 20 684)	.003 to 0.004	8	50 000 to 55 000	(34 474 to 37 921)	.008 to 0.009
4	30 000 to 35 000	(20 684 to 24 132)	.004 to 0.005	9	55 000 to 60 000	(37 921 to 41 368)	.009 to 0.010
				*	----------	----------	Above 0.010

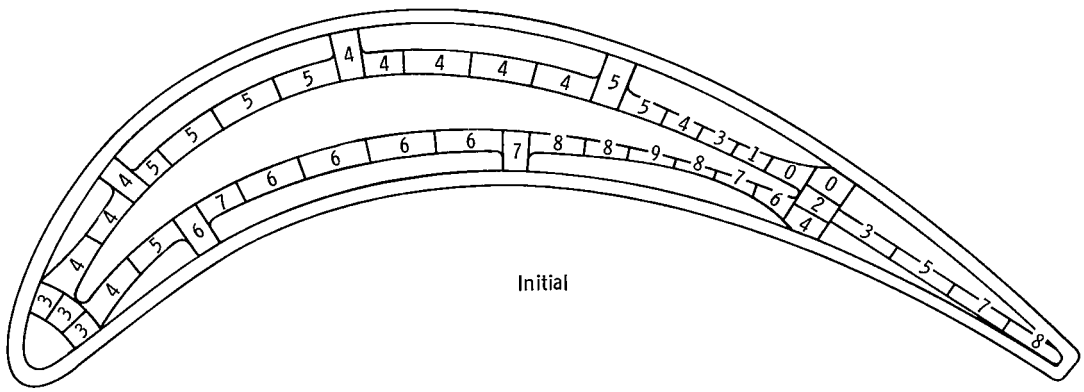

Initial

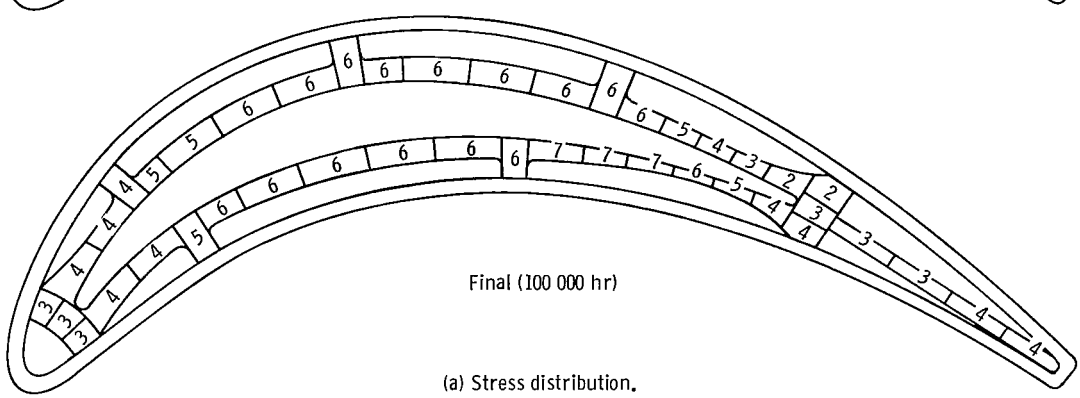

Final (100 000 hr)

(a) Stress distribution.

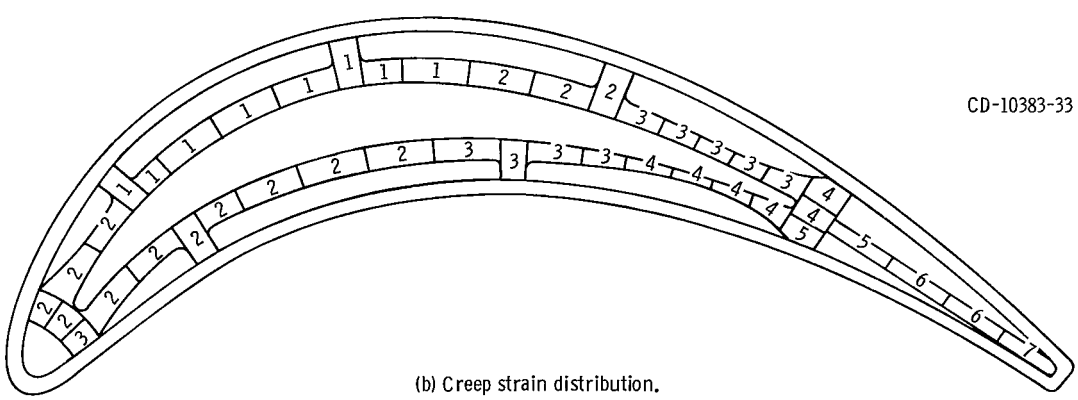

CD-10383-33

(b) Creep strain distribution.

Figure 14. - Stress analysis results for transpiration cooled design.

Key	Stress		Creep strain,	Key	Stress		Creep strain,
	psi	(N/cm^2)	in./in.		psi	(N/cm^2)	in./in.
0	Under 15 000	(Under 10 342)	Under 0.001	5	35 000 to 40 000	(24 132 to 27 579)	0.005 to 0.006
1	15 000 to 20 000	(10 342 to 13 790)	0.001 to 0.002	6	40 000 to 45 000	(27 579 to 31 026)	.006 to 0.007
2	20 000 to 25 000	(13 790 to 17 237)	.002 to 0.003	7	45 000 to 50 000	(31 026 to 34 474)	.007 to 0.008
3	25 000 to 30 000	(17 237 to 20 684)	.003 to 0.004	8	50 000 to 55 000	(34 474 to 37 921)	.008 to 0.009
4	30 000 to 35 000	(20 684 to 24 132)	.004 to 0.005	9	55 000 to 60 000	(37 921 to 41 368)	.009 to 0.010
				*	----------	----------	Above 0.010

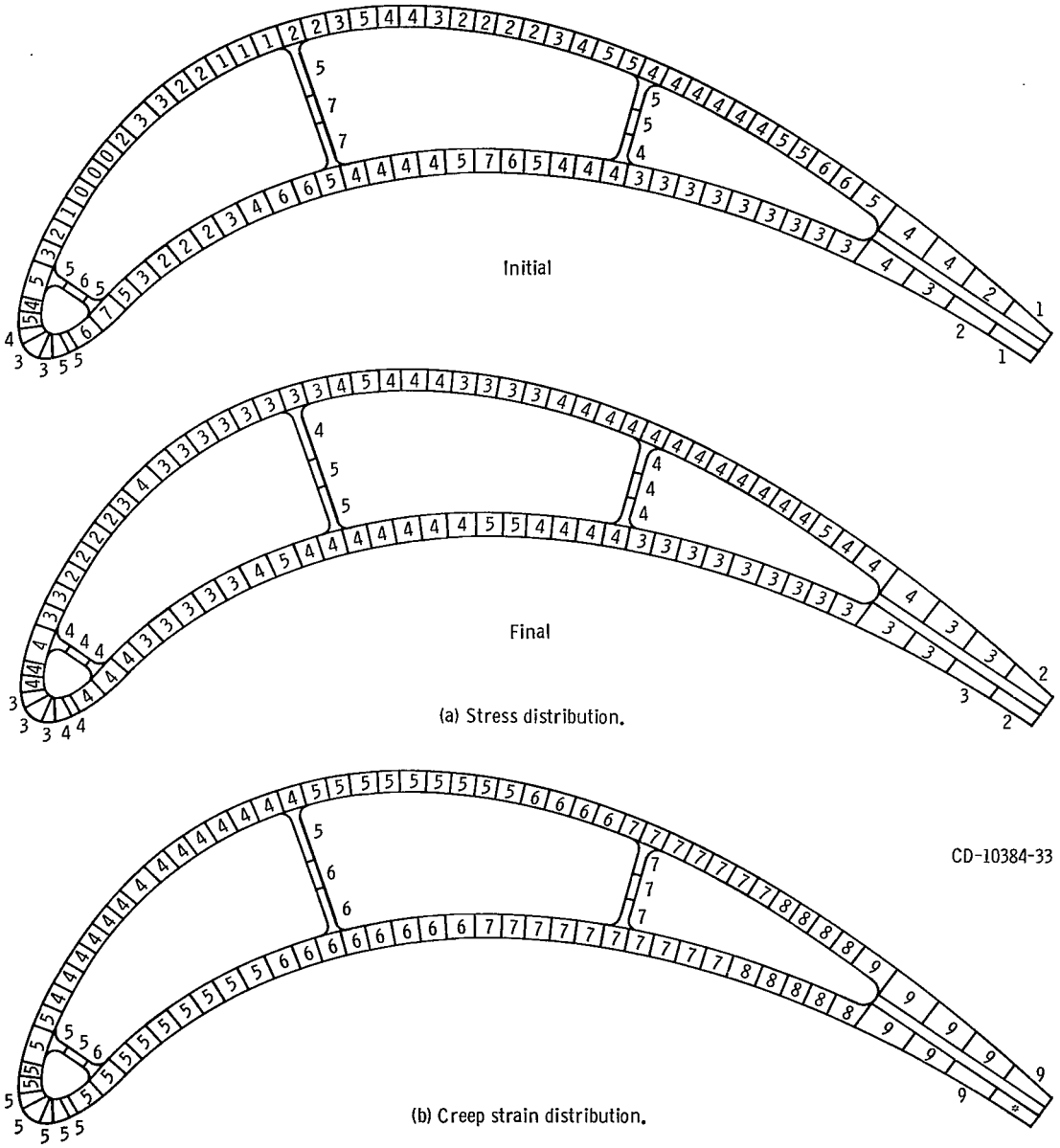

(a) Stress distribution.

(b) Creep strain distribution.

Figure 15. - Stress analysis results for multiple small hole design.

Key	Stress		Creep strain,
	psi	(N/cm^2)	in./in.
0	Under 15 000	(Under 10 342)	Under 0.001
1	15 000 to 20 000	(10 342 to 13 790)	0.001 to 0.002
2	20 000 to 25 000	(13 790 to 17 237)	.002 to 0.003
3	25 000 to 30 000	(17 237 to 20 684)	.003 to 0.004
4	30 000 to 35 000	(20 684 to 24 132)	.004 to 0.005
5	35 000 to 40 000	(24 132 to 27 579)	0.005 to 0.006
6	40 000 to 45 000	(27 579 to 31 026)	.006 to 0.007
7	45 000 to 50 000	(31 026 to 34 474)	.007 to 0.008
8	50 000 to 55 000	(34 474 to 37 921)	.008 to 0.009
9	55 000 to 60 000	(37 921 to 41 368)	.009 to 0.010
*	----------	----------	Above 0.010

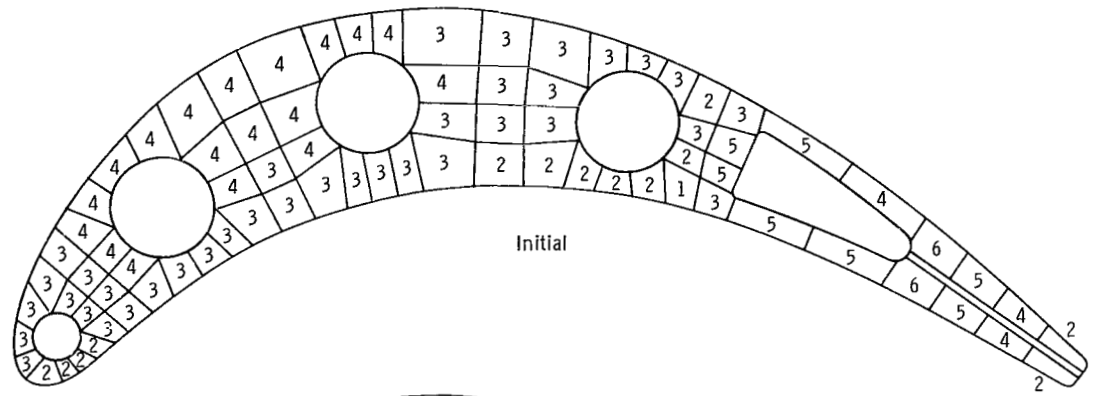

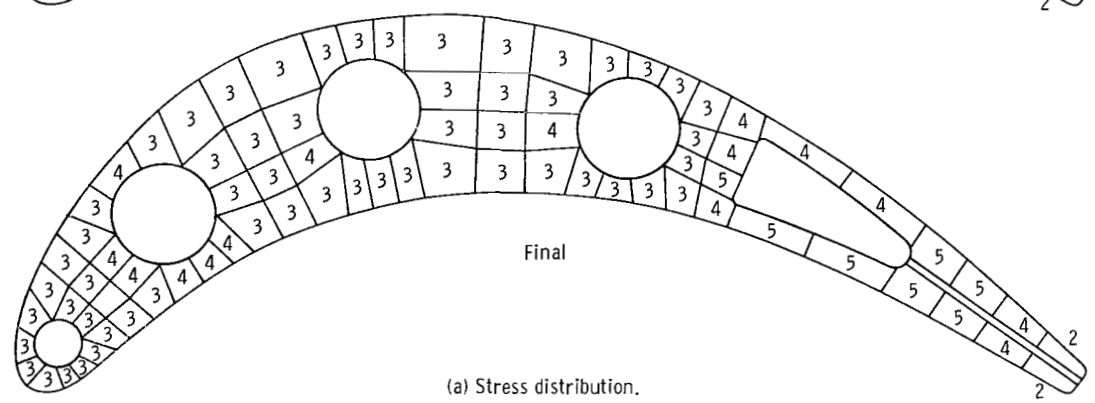

(a) Stress distribution.

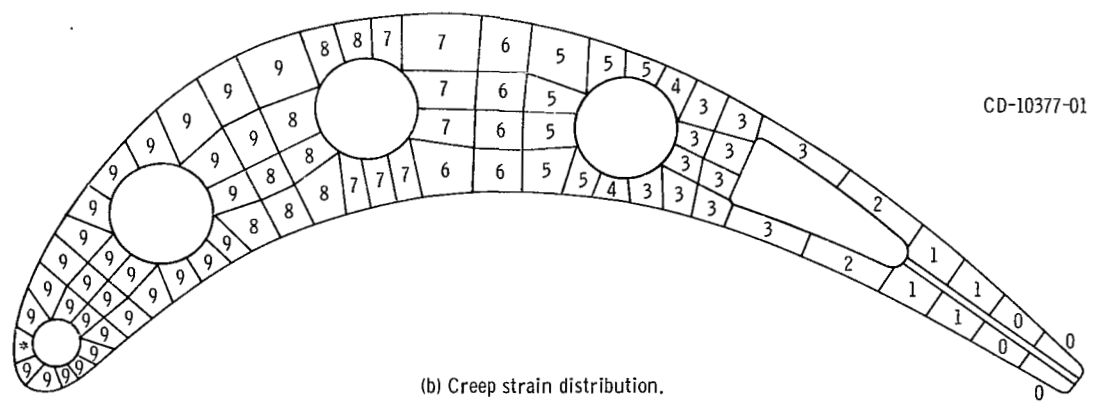

(b) Creep strain distribution.

Figure 16. - Stress analysis results for liquid-metal- and convection-cooled design.

Transpiration cooled design. - The trailing edge of the strut developed the highest creep strain. This was despite the sharp stress relaxation at the trailing edge projection shown in figure 14(a). Aside from this region, the creep strains in the strut appeared fairly well balanced (fig. 14(b)). Transpiration cooling requires a porous mesh material which will be resistant to oxidation at the 1600° F (1144 K) metal temperature. Otherwise the stress relaxation results for this design would be rather academic since oxidation would progressively close the fine pores and change the metal temperatures during steady-state operation.

Multiple small hole design. - This configuration had the highest creep life next to the transpiration cooled design. Of all the designs it had the best strain balance between leading and trailing edges as shown in figure 15(b) and is the closest to being optimized from a creep rupture standpoint. This balanced strain distribution was a result of the effect of creep in relaxing the leading edge and web stresses and raising the trailing edge stresses (fig. 15(a)). These relaxation effects are so complicated that the only way to deliberately design the blade with an optimum coolant flow distribution to give the maximum creep life would be by a trial and error procedure using a stress relaxation analysis. However, under some conditions where the creep life is considerably more than required for the design life of the blade, it may be desirable to redistribute the coolant to lower the temperatures of other potential problem areas such as the leading edge in the midspan region which may have a low cycle fatigue problem.

Liquid metal and convection cooled design. - The highest stresses generally occurred adjacent to the coolant feed channels near the leading and trailing edges. Figure 16(a) shows only a relatively small relaxation of these stresses. The creep strain distribution in figure 16(b) is badly balanced with the trailing edge showing virtually no creep. This design could be improved somewhat by using less air to cool the trailing edge and more to improve the heat exchanger efficiency.

Multiple Small Hole Blade Design Curves

Curves of percent coolant to total flow against average blade metal temperatures for the multiple small hole configuration are shown in figure 17 for turbine inlet gas temperatures of 2270° F (1517 K) and 2570° F (1683 K) with a blade coolant inlet temperature of 1270° F (961 K) which was used in references 1 to 3 for the previous design cases. Curves are also shown for a 2570° F (1683 K) turbine inlet gas temperature with 1000° F (811 K) and 600° F (589 K) coolant blade inlet temperatures. These curves were established from analytical temperature data given in reference 2 and, where these were not available, by using the transpiration cooling effectiveness parameter derived in reference 2 even though this is a film cooling design. It was found that this param-

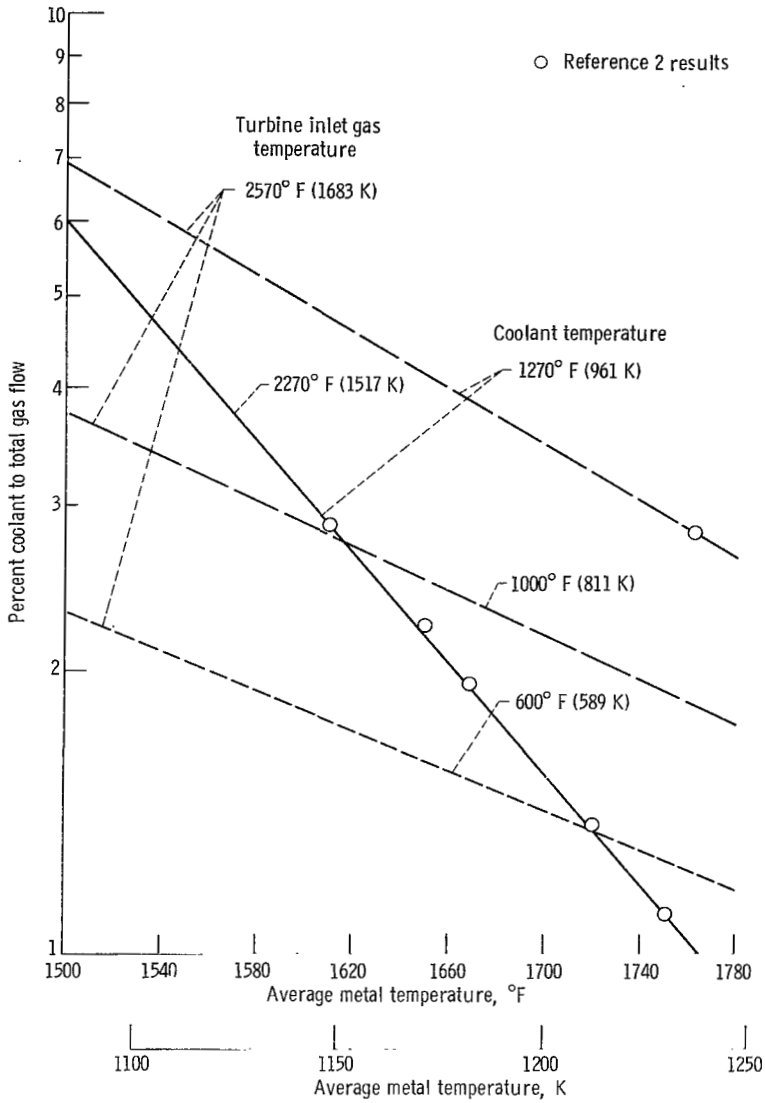

Figure 17. - Effect of turbine gas inlet and coolant temperatures on metal temperature for multiple small hole design. Cruise condition: altitude, 75 000 feet (km); speed, Mach 3.

eter gave a better correlation with the analytical data shown in figure 17 than the more frequently used convective cooling effectiveness parameter. Metal temperature for other conditions can be determined in a similar manner.

Curves of creep lives as a function of average metal temperatures are presented in figure 18 for centrifugal stress levels of 20 000, 24 000, and 30 000 psi (13 790, 16 547, and 20 684 N/cm^2) for the multiple small hole design. Results for other centrifugal stresses can be obtained by cross plotting the curves.

These curves were determined by (1) raising all the nodal temperatures of fig-

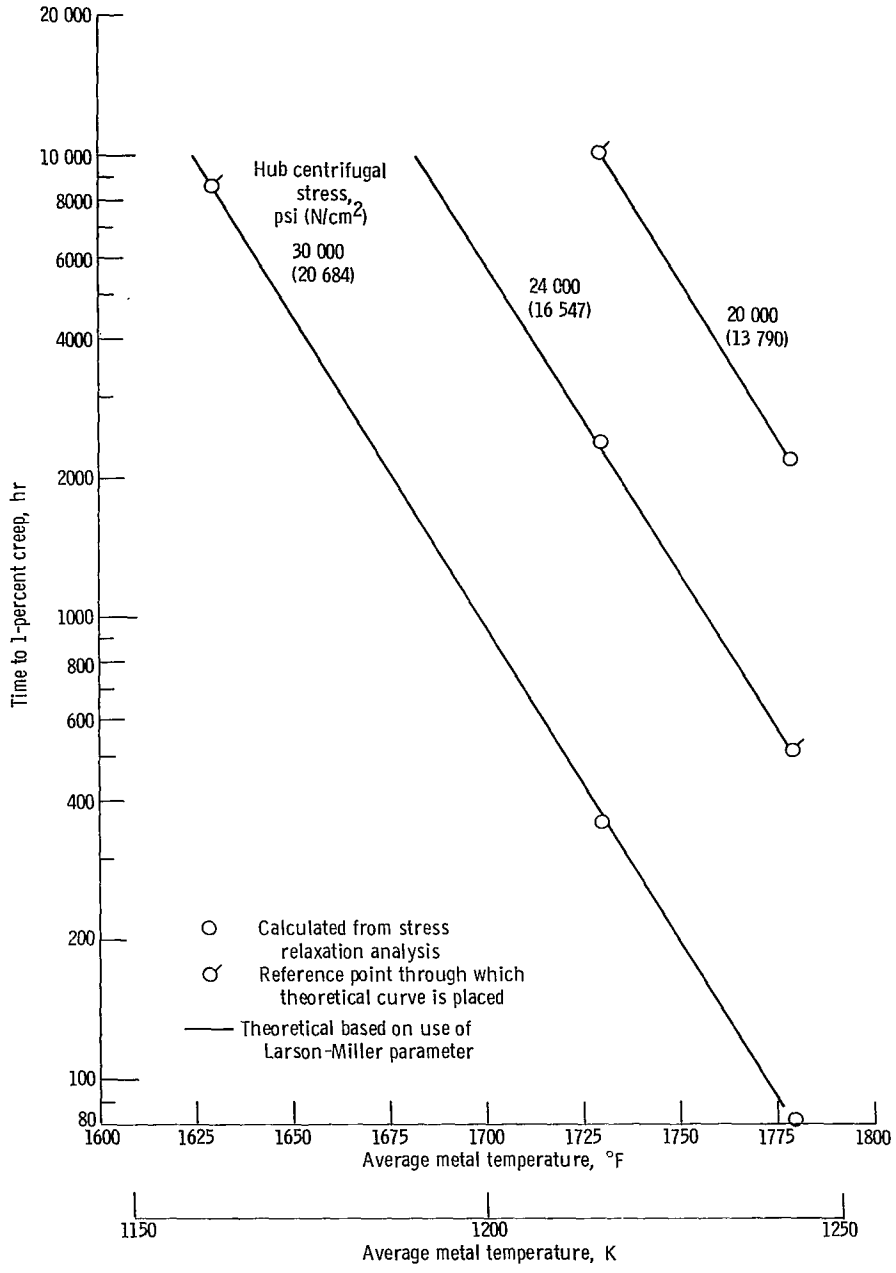

Figure 18. - Effect of metal temperature on creep life of multiple small hole design.

ure 9 (p. 18) by an amount equal to the difference between the new blade average metal temperature and the previous one of 1629° F, (2) applying the desired centrifugal stress level and recomputing the creep life from the stress relaxation analysis for one reference case, (3) calculating an effective Larson-Miller parameter, $T_R(25.56 + \log_{10}t)$, based on this case, and (4) using the effective parameter to calculate the time to failure at any other metal temperature. In this way, the theoretical curves of figure 18 were established. The creep lives for a number of other cases at various centrifugal stresses and metal temperature levels were computed directly from the stress relaxation analysis and are shown by data points in figure 18. As can be seen agreement with the theoretical curve was excellent. In all the cases recomputed for other temperature levels, the final creep strain distribution remained essentially unchanged. The design curves of figure 18 do not include the effect of the centrifugal force restoring moments due to bending.

As an example of how the design curves can be used, the conditions required to attain a 1000 hour life at a turbine gas inlet temperature of 2570° F (1683 K) with a 30 000 psi (20 684 N/cm^2) centrifugal stress will be examined. From figure 18 it is found that an average metal temperature of about 1700° F (1200 K) is required for 1000 hours life at 30 000 psi (20 684 N/cm^2). In figure 17 it is seen that combinations of coolant to total flow and coolant temperatures which will give 1700° F (1200 K) are 3.45 percent of 1270° F (961 K) air, 2.18 percent of 1000° F (811 K) air, and 1.42 percent of 600° F (589 K) air. Another example is to consider the effect on blade life of increasing the turbine inlet temperature from 2270° to 2570° F (1517 to 1683 K) while using 2.8 percent coolant at 1270° F (961 K) with a 30 000 psi (20 684 N/cm^2) centrifugal stress. This increases the average metal temperature from 1615° to 1761° F (1153 to 1234 K) (fig. 17) and reduces the life from over 10 000 to 140 hours (fig. 18). If the centrifugal stress level for the 2570° F (1683 K) condition is 20 000 psi (13 790 N/cm^2) instead of 30 000 psi(20 684 N/cm^2), the life increases to 3800 hours or about 27 times for a 33 percent reduction in stress level.

As a check on these design curves a 2570° F (1683 K) turbine inlet temperature case with a 30 000 psi (20 684 N/cm^2) centrifugal stress was analyzed using the temperature distribution given in reference 2 for a 2.8 percent coolant to total gas flow. The analytical creep life was 70 hours compared to 138 hours that would be predicted on the basis of figures 17 and 18. The shorter analytical life was due mainly to a final unbalanced creep strain distribution which had most of the creep occurring at the trailing edge and little at the leading edge. Another factor which serves to make the results in figure 18 somewhat unconservative is that the analytical temperature distributions of reference 2 show a tendency for the temperature difference to increase with increasing turbine inlet temperature. However, little effect on the temperature difference is shown in reference 2 when the turbine inlet temperature is kept constant but the coolant flow rate is changed.

CONCLUDING REMARKS

This analysis does not take thermal fatigue into account and, therefore, does not consider the effects of discontinuities such as film cooling holes and fin to shell junctions in reducing the cyclic lives of the blades. The influence of these discontinuities depends on factors such as their geometries, the thermal and mechanical stress fields, coupling due to strain gradients, and stress relieving effects due to arrays of openings or intersecting passages and to plastic flow. Consideration of these effects is beyond the present state of the art of turbine blade stress analysis except by empirical methods based on extensive experimental results. The transpiration cooled blade which showed the longest creep life requires a porous material which could provide the fine passages required for ideal transpiration cooling and still tolerate thousands of hours of operation at 1600° F (1144 K). Otherwise, long before the theoretical creep life could be reached the porous skin would undergo progressive oxidation which would clog passages, restrict coolant flow, increase metal temperatures, and accelerate further oxidation. Up to the present time transpiration cooling 1000 hours of steady state operation has not been feasible for metal temperatures much beyond 1600° F (1144 K). However, development of more oxidation resistant materials or coatings for porous shells could enable this cooling method to be used for much higher skin temperatures. Another problem that could limit the lives of strut supported transpiration cooled blades is the difficulty of obtaining a strong reliable joint at the shell to strut interface. Weak joints would be susceptible to thermal stress fatigue.

The multiple small hole blade showed the best creep life next to the transpiration cooled blade and would appear to be the most promising of the designs for long time steady-state operation with high metal temperature levels at the present time. The main reason for its superiority over the strut insert and film-convection blades was the more uniform temperature distribution at the hub section. However, the results of references 1 to 3 demonstrated that all three of these designs had fairly close overall temperature levels and temperature differences over the airfoil surfaces. Thus, for the 2.6 percent coolant flow ratio the range of maximum temperature differences over the shell was 245° to 301° F (136 to 167 K) and the average shell temperatures ranged from 1629° to 1653° F (1160 to 1174 K) for these designs. The steady-state lives depend on the mechanical loads, temperature levels, and temperature gradients. It therefore appears possible that, neglecting fabrication problems, these three blade configurations could be designed to possess approximately the same steady-state operating lives if the wall temperature distributions were optimized. Therefore, the creep life for the multiple small-hole blade may indicate what the strut insert and film-convection cooled blade also attain. However, the 4 or 5 to 1 ratio between the creep lives of the multiple small hole and film-convection blades, despite a lower centrifugal stress assigned to

the latter, demonstrates the drastic effect on blade life that can occur as a result of differences in metal temperature distributions.

Since the results of the heat transfer analyses of references 1 to 3 show only a small effect of configuration geometry for the three basic configurations cited above it would seem that, as long as the coolant can be effectively dispersed around the blade, the selection of a configuration should depend largely on considerations of structure, fabrication, aerodynamics, and, perhaps, cyclic life. From structural and fabrication standpoints the strut insert design may not be desirable because of the horizontal fins which are dead weight and difficult to cast. Since both the multiple small hole and film and convection cooled blades possess arrays of holes near both leading and trailing edges there may be little to choose between them from aerodynamic and cyclic life standpoints.

The liquid metal design had the lowest creep life because of the high metal temperature level at the hub section. This configuration had a higher overall blade temperature of approximately 100° F (56 K) compared to the multiple small hole, strut insert, and film-convection cooled configurations for the same amount of compressor discharge air. Therefore, this configuration could not be improved qualitatively by improving the temperature distribution. The higher metal temperatures probably result from added losses by not using the compressor discharge air to cool the blade directly. Instead, most of the air was used to cool the heat exchanger tubes and condense the potassium. A better heat exchanger design would improve the blade life. However, this design has other obvious problems. The centrifugal loads of the relatively heavy blades together with the large amount of material which has to be removed at the rotor rim for the heat exchangers would require a thicker and, therefore, heavier rotor. At first inspection the liquid metal concept does not appear too appealing.

A reasonable goal for the operating lives of turbine blades for advanced airbreathing engines would be 1000 hours. All of the blade designs except the liquid metal configuration met this requirement for the Mach 3, 75 000 feet (22 859 km), 2270° F (1517 K) turbine gas inlet temperature engine cruise conditions. The multiple small hole blade, in particular, had such excessive creep life for these conditions that it might be beneficial to decrease it by letting the leading edge run colder and the trailing edge hotter. This would probably help the fatigue life of the leading edge region which could be a more life limiting factor than the steady-state operation.

From the design curves of figures 17 and 18 about 3.5 percent coolant to total gas flow would be required for the multiple small hole blade to have 1000 hours life at a 2570° F (1683 K) turbine gas inlet temperature under cruise conditions with a 30 000 psi (20 684 N/cm^2) centrifugal stress. It might seem that this blade life could be increased by doing more cooling near the blade base and less above the midspan region. However, the analytical results of references 1 to 3 show metal temperatures above 1800° F (1255 K) and sometimes as high as 1900° F (1311 K) in the midspan to tip regions.

These temperatures are already dangerous from both structural and oxidation considerations and cannot be raised further without compromising the blade integrity.

It should be emphasized that the design curves of figures 18 are an indication only of the blade potential. They presuppose a coolant distribution which will give an evenly balanced creep strain distribution between leading and trailing edge. From an analytical standpoint this would be difficult to achieve since the stress relaxation process is extremely complex and it is not obvious what initial stress distribution to design for. Even if this could be determined by a trial and error procedure using a stress relaxation program, problems involved in fabrication, oxidation effects during operation, variations in gas temperature profile with combustor location, errors in determining blade gas pressure distributions, etc., could make this impossible to attain in practice. It, therefore, is probably necessary to either design for a safety factor on life or to design for a deliberately unbalanced creep strain distribution.

CONCLUSIONS

The following conclusions were drawn from the analytical investigation of the steady-state operating creep lives of five turbine blade cooling designs for advanced airbreathing engines:

1. The longest creep life was shown by the transpiration cooled design neglecting oxidation problems with the porous shell and a possible thermal fatigue problem at the shell to strut joint.

2. The multiple small hole design showed significantly longer life than the strut insert and film-convection cooled designs. The temperature distribution across the hub section was the main factor in determining the ranking of these three blade designs. All these blades were relatively close in centrifugal stresses, average temperature levels, and overall blade maximum temperature differences. It therefore appears that the differences in temperature distribution have drastic effects and that it may be possible to design the strut insert and film and convection cooled blades to have about the same creep lives as the multiple small hole blade if their temperature distributions were optimized for the engine design conditions.

3. The liquid metal blade design had the worst creep life of the designs which were studied. The bulk and complexity of the heat exchanger did not result in any advantage in life.

4. All the blade configurations but the liquid metal design showed steady-state lives in excess of 1000 hours for the Mach 3, 75 000 feet (22.859 km), 2270° F (1517 K) turbine inlet temperature advanced airbreathing engine design conditions which were considered. The multiple small hole design also had the capability of operating at 2570° F

(1683 K) turbine inlet temperature with a small rise in coolant flow.

5. Raising the web temperatures of the film and convection cooled blade to those of the adjoining parts of the shell only lowered the creep life. This was because the average temperature level at the hub section increased and caused a slower stress relaxation to occur at the critical trailing edge.

6. The creep lives of the configurations cannot be determined either qualitatively or quantitatively from the initial or the average conditions of stress and temperature. Stress relaxation causes the higher thermal stresses to decrease, changes the stress distribution and, therefore, the creep rates, and sometimes causes a shift in the critical region of the airfoil section.

7. Failure to consider the restoring moments due to centrifugal force as the blades bend because of creep can result in calculated lives which are overly conservative. The application of this correction to the stress relaxation analysis caused an increase in life for all the blade designs although by varying amounts. The transpiration cooled blade life increased from 47 900 hours to an infinite life. On the other hand, the liquid metal blade showed only a minor increase in life. The qualitative ranking of the designs was not affected by the correction.

8. The theoretical effect of an increase in the average metal temperature level can be predicted using the Larson-Miller parameter if the life at only one average temperature level is known, provided neither the centrifugal stress nor the temperature distribution is changed.

Lewis Research Center,
National Aeronautics and Space Administration,
Cleveland, Ohio, February 10, 1969,
720-03-00-74-22.

APPENDIX A

STRESS RELAXATION ANALYSIS

The usual assumption of strain compatability is made that plane sections remain plane. For a blade with three degrees of freedom, the total normal strain is defined by

$$\epsilon_t = C_1 + C_2 y + C_3 x \tag{A1}$$

where C_1, C_2, and C_3 are the intercepts and slopes of the plane.

The total strain on any element consists of (1) the elastic strain σ_{zk}/E_k, (2) the thermal deformation $\alpha_k T_k$, (3) the residual strain from previous plastic flow or the plastic component of strain ϵ_{pk}, and (4) the total accumulated creep strain ϵ_{ck}. Therefore, the total strain at any time is

$$\epsilon_{tk} = \frac{\sigma_{zk}}{E_k} + \alpha_k T_k + \epsilon_{pk} + \epsilon_{ck} \tag{A2}$$

or

$$\sigma_{zk} = E_k(\epsilon_{tk} - \alpha_k T_k - \epsilon_{pk} - \epsilon_{ck}) \tag{A3}$$

Substitution of (A1) into (A3) gives the compatibility equation

$$\sigma_{zk} = E_k(C_1 + C_2 y_k + C_3 x_k - \alpha_k T_k - \epsilon_{pk} - \epsilon_{ck}) \tag{A4}$$

The boundary conditions are

$$\iint \sigma_{zk}\, dx\, dy = F \tag{A5}$$

$$\iint \sigma_{zk} y_k\, dx\, dy = M_x \tag{A6}$$

$$\iint \sigma_{zk} x_k\, dx\, dy = M_y \tag{A7}$$

The applied moments M_x and M_y consist of components with respect to the coordinate axes of moments due to both gas and centrifugal forces. These moments are positive when they cause an increasing stress with increasing values of x or y.

Substitution of (A4) into (A5) to (A7) gives equations (A8) to (A10), respectively

$$\iint (C_1 + C_2 y + C_3 x - \alpha T - \epsilon_p - \epsilon_c) E \, dx \, dy = F \tag{A8}$$

$$\iint (C_1 + C_2 y + C_3 x - \alpha T - \epsilon_p - \epsilon_c) Ey \, dx \, dy = M_x \tag{A9}$$

$$\iint (C_1 + C_2 y + C_3 x - \alpha T - \epsilon_p - \epsilon_c) Ex \, dx \, dy = M_y \tag{A10}$$

or equations (A11) to (A13), respectively.

$$C_1 \iint E \, dA + C_2 \iint Ey \, dA + C_3 \iint Ex \, dA = F + \iint (\alpha T + \epsilon_p + \epsilon_c) E \, dA \tag{A11}$$

$$C_1 \iint Ey \, dA + C_2 \iint Ey^2 dA + C_3 \iint Exy \, dA = M_x + \iint (\alpha T + \epsilon_p + \epsilon_c) Ey \, dA \tag{A12}$$

$$C_1 \iint Ex \, dA + C_2 \iint Exy \, dA + C_3 \iint Ex^2 dA = M_y + \iint (\alpha T + \epsilon_p + \epsilon_c) Ex \, dA \tag{A13}$$

These equations can be further simplified if the coordinate axes are converted to centroidal axes where the centroid is defined by $\int Ex \, dA = \int Ey \, dA = 0$ and the axes are defined by $\int Exy \, dA = 0$. The equations for converting from the arbitrary set of axes to centroidal axes are given by equations (A14) to (A18) where equations (A14) to (A16) are based on reference 6.

$$\bar{x} = \frac{\iint Ex \, dA}{\iint E \, dA} \tag{A14}$$

$$\bar{y} = \frac{\iint Ey \, dA}{\iint E \, dA} \tag{A15}$$

$$\theta = \frac{1}{2}\tan^{-1}\left[\frac{2\left(\iint Exy\ dA - \overline{xy}\iint E\ dA\right)}{\iint Ex^2 dA - \overline{x}^2\iint E\ dA - \iint Ey^2 dA + \overline{y}^2\iint E\ dA}\right] \tag{A16}$$

$$x'_k = (x_k - \overline{x})\cos\theta + (y_k - \overline{y})\sin\theta \tag{A17}$$

$$y'_k = (y_k - \overline{y})\cos\theta - (x_k - \overline{x})\sin\theta \tag{A18}$$

If x_k and y_k are replaced by x'_k and y'_k the coefficients C_1, C_2, and C_3 can be solved from equations (A19) to (A21).

$$C_1 = \frac{F + \iint(\alpha T + \epsilon_p + \epsilon_c)E\ dA}{\iint E\ dA} \tag{A19}$$

$$C_2 = -\frac{M'_x + \iint(\alpha T + \epsilon_p + \epsilon_c)Ey'\ dA}{\iint E(y')^2 dA} \tag{A20}$$

$$C_3 = \frac{M'_y + \iint(\alpha T + \epsilon_p + \epsilon_c)Ex'\ dA}{\iint E(x')^2 dA} \tag{A21}$$

Substitution of equations (A19) to (A21) into (A4) gives σ_{zk} which in summation form is

$$\sigma_{zk} = E_k \left[\frac{F + \sum_{k=1}^{n} (\alpha_k T_k + \epsilon_{pk} + \epsilon_{ck}) E_k \, \Delta A_k}{\sum_{k=1}^{n} E_k \, \Delta A_k} \right]$$

$$+ y' E_k \left[\frac{M'_x + \sum_{k=1}^{n} (\alpha_k T_k + \epsilon_{pk} + \epsilon_{ck}) E_k y'_k \, \Delta A_k}{\sum_{k=1}^{n} E_k (y'_k)^2 \, \Delta A_k} \right]$$

$$+ x' E_k \left[\frac{M'_y + \sum_{k=1}^{n} (\alpha_k T_k + \epsilon_{pk} + \epsilon_{ck}) E_k x'_k \, \Delta A_k}{\sum_{k=1}^{n} E_k (x'_k)^2 \, \Delta A_k} \right] - E_k (\alpha_k T_k + \epsilon_{pk} + \epsilon_{ck}) \qquad \text{(A22)}$$

The strain hardening rule requires that the change in creep strain over a time interval Δt, be determined at a constant stress which is calculated from the previous accumulated creep strain. Stresses are calculated from equation (A22) and creep strains from equation (1). The procedure is as follows:

(1) Calculate σ_{zk} from equation (A22). This process is started at $t = 0$ hours where $\epsilon_{ck} = 0$.

(2) Compute a fictitious value of time t' for each node by solving equation (1) for t' using σ_{zk} from step 1 with the same ϵ_{ck} used in step 1.

(3) Solve for the new creep strain ϵ_{ck} at the end of the next time interval by substituting $t' + \Delta t$ for t in equation (1).

(4) Go back to step 1 using the new ϵ_{ck}.

This procedure is repeated over successive time intervals until a creep strain limit is reached. The total elapsed time is the sum of all the time increments which were applied. Small time increments are used in order to apply an incremental method.

APPENDIX B

ANALYSIS OF RESTORING MOMENTS DUE TO CREEP

The blade centrifugal force distribution in the spanwise direction was approximated by

$$F_z = F_{z,o}\left[1 - 0.6\left(\frac{z}{L}\right) - 0.4\left(\frac{z}{L}\right)^2\right] \tag{B1}$$

The curvature at any span location is assumed to be defined by

$$\frac{1}{R} = \frac{1}{R_o}\left(\frac{z}{L} - 1\right)^2 \tag{B2}$$

The usual approximation for curvature is made that

$$\frac{1}{R} = \frac{d^2w}{dz^2} \tag{B3}$$

The second and first derivatives of the deflection along the blade span are then given by

$$\frac{d^2w}{dz^2} = \frac{1}{R_o}\left[\left(\frac{z}{L}\right)^2 - 2\left(\frac{z}{L}\right) + 1\right] \tag{B4}$$

$$\frac{dw}{dz} = \frac{L}{R_o}\left[\frac{1}{3}\left(\frac{z}{L}\right)^3 - \left(\frac{z}{L}\right)^2 + \left(\frac{z}{L}\right)\right] \tag{B5}$$

The restoring moment due to the centrifugal force is

$$M = -\int F_z \, dw \tag{B6}$$

Substitution of equations (B1) and (B5) into (B6) yields

$$M = -\frac{F_{z,o}L}{R_o}\int_0^L \left[-0.133\left(\frac{z}{L}\right)^5 + 0.200\left(\frac{z}{L}\right)^4 + 0.533\left(\frac{z}{L}\right)^3 - 1.600\left(\frac{z}{L}\right)^2 + \frac{z}{L}\right]dz \tag{B7}$$

which results in

$$M = -0.118\,\frac{F_{z,o}L^2}{R_o} \tag{B8}$$

Since $1/R_o$ is equivalent to the slope of the hub section, the restoring moments become

$$M_x = -0.118\,F_{z,o}L^2C_2 \tag{B9}$$

and

$$M_y = -0.118\,F_{z,o}L^2C_3 \tag{B10}$$

REFERENCES

1. Burggraf, F.; Murtaugh, J, P.; and Wilton, M. E.: Design and Analysis of Cooled Turbine Blades. Part II - Convection Cooled Nozzles and Buckets. Rep. R68AEG102, General Electric Co. (NASA CR-54514), Jan. 1, 1968.

2. Burggraf, F.; Murtaugh, J. P.; and Wilton, M. E.: Design and Analysis of Cooled Turbine Blades. Part III - Transpiration and Multiple Small Hole Film Cooled Nozzles and Buckets. Rep. R68AEG103, General Electric Co. (NASA CR-54515), Jan. 1, 1968.

3. Burggraf, F.; Murtaugh, J. P.; and Wilton, M. E.: Design and Analysis of Cooled Turbine Blades. Part IV - Combined Methods of Cooling. Rep. R68AEG104, General Electric Co. (NASA CR-54512), Jan. 1, 1968.

4. Danforth, C. E.; and Burggraf, F.: Design and Analysis of Cooled Turbine Blades. Part V - Life Prediction of Selected Designs. Rep. R68AEG105, General Electric Co. (NASA CR-72417), Aug. 1968.

5. Mendelson, Alexander; Roberts, Ernest, Jr.; and Manson, S. S.: Optimization of Time-Temperature Parameters for Creep and Stress Rupture, with Application to Data from German Cooperative Long-Time Creep Program. NASA TN D-2975, 1965.

6. Gendler, Sel; and Johnson, Donald F.: Determination of Minimum Moments of Inertia of Arbitrarily Shaped Areas, Such as Hollow Turbine Blades. NACA RM E9H10, 1950.

NASA-Langley, 1969 —— 28 E-4650

"The aeronautical and space activities of the United States shall be conducted so as to contribute . . . to the expansion of human knowledge of phenomena in the atmosphere and space. The Administration shall provide for the widest practicable and appropriate dissemination of information concerning its activities and the results thereof."

—NATIONAL AERONAUTICS AND SPACE ACT OF 1958

NASA SCIENTIFIC AND TECHNICAL PUBLICATIONS

TECHNICAL REPORTS: Scientific and technical information considered important, complete, and a lasting contribution to existing knowledge.

TECHNICAL NOTES: Information less broad in scope but nevertheless of importance as a contribution to existing knowledge.

TECHNICAL MEMORANDUMS: Information receiving limited distribution because of preliminary data, security classification, or other reasons.

CONTRACTOR REPORTS: Scientific and technical information generated under a NASA contract or grant and considered an important contribution to existing knowledge.

TECHNICAL TRANSLATIONS: Information published in a foreign language considered to merit NASA distribution in English.

SPECIAL PUBLICATIONS: Information derived from or of value to NASA activities. Publications include conference proceedings, monographs, data compilations, handbooks, sourcebooks, and special bibliographies.

TECHNOLOGY UTILIZATION PUBLICATIONS: Information on technology used by NASA that may be of particular interest in commercial and other non-aerospace applications. Publications include Tech Briefs, Technology Utilization Reports and Notes, and Technology Surveys.

Details on the availability of these publications may be obtained from:

SCIENTIFIC AND TECHNICAL INFORMATION DIVISION

NATIONAL AERONAUTICS AND SPACE ADMINISTRATION

Washington, D.C. 20546